dent calcium channels can be activated following the binding of a ligand to receptors on the cell surface. Furthermore, both receptor-linked GTP-binding proteins and second-messenger systems within the cytosol can affect the activity of ion channels. Thus, complex regulatory pathways linking surface receptors, the metabolism of the cell and ion channels can result in long-lasting changes in the behavior of the cell.

The patch clamp technique provides the experimental means for merging the tools of modern molecular and cellular biology with those of electrophysiology. Using the various recording configurations, it is possible to dissect the mechanisms of channel modulation. In cell-attached recording, modulation of channel activity in response to bath-applied agonist generally indicates a second-messenger mechanism. Candidate messengers can be tested directly on excised patches or in whole-cell recording. Perforated patch recording maintains the integrity of second-messenger systems while enabling the overall activity of ion channels in the cell to be evaluated following receptor stimulation. Current research on signaling pathways seeks to establish the functionally meaningful mechanisms through selective activation or inhibition of a portion of the pathway. The variety of patch clamp configurations, combined with single-channel resolution, provides a powerful experimental approach from the molecular level, in which channel genes are altered and expressed, to the cellular level, in which posttranslational signaling mechanisms are elucidated, to the systems level, in which cellular interactions in intact or slice preparations are revealed.

[2] Constructing A Patch Clamp Setup

By RICHARD A. LEVIS and JAMES L. RAE

Basic Components in Patch Clamp Setup

Different investigators have chosen to construct their patch clamp setups in very different ways, and it is clear that there is no one "best" way to configure the apparatus for patch clamping. There are, however, many features that good setups have in common, and there are some basic principles that one should consider when configuring and purchasing patch clamp hardware.[1,2] In this chapter we discuss these principles, describe

[1] J. L. Rae and R. A. Levis, *Mol. Physiol.* **6**, 115 (1984).
[2] J. L. Rae, R. A. Levis, and R. S. Eisenberg, *in* "Ion Channels" (T. Narahashi, ed.), p. 283. Plenum, New York and London, 1988.

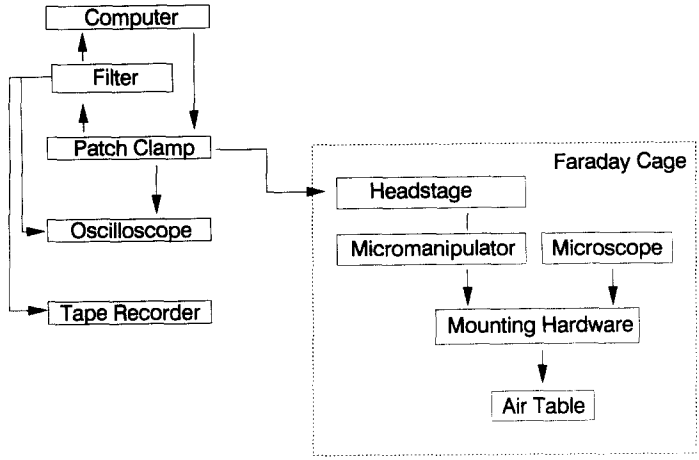

FIG. 1. Block diagram for a patch clamp setup.

ways in which investigators have implemented them, and suggest procedures that can result in very high quality patch clamp recordings.

Figure 1 shows a block diagram of a patch clamp setup that includes the important elements that any set should have. In the sections that follow, we take each of the elements from this diagram and discuss ways in which they might be implemented in a working patch clamp setup. We particularly emphasize the electronics and low noise techniques since it is through understanding these aspects of patch clamping that an investigator can most markedly improve the technical quality of the recordings.

The Microscope

Because the majority of patch clamp studies have been done on single cultured cells or on single freshly dissociated cells, inverted microscopes have been utilized most often. With these microscopes, visualization occurs from the side opposite to that from which the electrodes are positioned. With this arrangement, it is possible to use condensers whose working distance is sufficiently long that the patch clamp headstage, electrode holder, and electrode easily fit under the condenser with little worry about making mechanical contact with it.

With inverted microscopes, it is also possible to utilize a chamber whose bottom is optically ideal and in very close proximity to the objective. This allows one to employ high numerical aperture (NA) objectives with maximum resolving power. It is, however, not possible in general to

make actual patch clamp measurements while utilizing the maximal resolving power (M_{res}) of the microscope. To do this would require the use of a condenser whose numerical aperture was as high as that of the objective since $M_{res} \cong 1.22\lambda_0/(NA_{obj} + NA_{cond})$ where λ_0 is the wavelength of light being used. High numerical aperture condensers do not have sufficiently long working distances that electrodes can fit under them. The long working distance condensers required have lower numerical aperture (0.6 or so) and thus lower resolution. Still, the total resolution of the microscope is quite good as long as the numerical aperture of the objective is large. Inverted microscopes also focus routinely by moving the nosepiece with its attached objective rather than by moving the stage. This offers the advantage that the chamber holding the cells can be rigidly attached to the stage for mechanical stability. In addition, it is often possible to mount the micromanipulators that hold the headstage and electrodes directly to the stage, an arrangement that is quite good mechanically. Other than these obvious advantages, there is little to recommend an inverted microscope over an upright microscope as both will accept the same wide range of accessories such as video cameras, photometers, and fluorescence attachments.

In some instances, preparations that have more than one cell layer must be utilized for patch clamping. With an inverted microscope, one is forced to look at the top layer of cells on which the patch clamping will be done through several layers of deep cells. This arrangement can cause substantial optical distortion at best and complete loss of visibility at worse. Under these circumstances, it is necessary to use an upright microscope with an objective that has a sufficiently long working distance that the patch electrodes and holder can be placed under the objective. Most microscope companies market a line of metallurgical objectives that have working distances in the 10–20 mm range while maintaining quite good numerical apertures. The Nikon (Garden City, NY) extralong working distance and super-long working distance objectives are most notable in this regard, although the 25× from Leitz (Rockleigh, NJ) is also an excellent choice. With these objectives, one can look directly at the surface of a multilayer preparation and have sufficient working distance to place an electrode on that cell layer under direct observation. In general, one must partially cover the chamber with a piece of microscope slide glass and place the electrode tip under it from the side. One then views the preparation through the microscope glass without the distortion caused by the meniscus of fluid that would otherwise exist near the edge of the electrode as shown in Fig. 2.

Most microscope companies are willing to make modifications to their microscopes in which a hinge is placed in the body of the microscope so that the binocular head and nosepiece can be folded back away from the

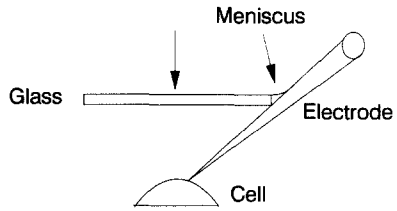

FIG. 2. Schematic drawing of the "glass bottom boat" approach for viewing cells from above with a noninverted compound microscope. The meniscus occurs at the edge of the glass and thus does not distort the field of vision.

chamber to give the investigator sufficient room for inserting the preparation in the chamber. If a long working distance, low power objective is used, microdissection can also be done as required. Figure 3 is a photograph of an inexpensive Nikon labophot modified in this way. This microscope utilizes an erect image binocular head which is imperative if one is to use it for microdissection.

Either inverted or upright microscopes have a variety of optical techniques available for visualizing the cells. Here again, inverted microscopes offer clear advantages optically both because of their ability to use short working distance, high numerical aperture objectives and because they can utilize the principle of transmitted light, Nomarski interference contrast. In this technique, when implemented with a high numerical aperture objective, an extremely thin optical slice is cut through the cell of interest with little interference from structures located either above or below the plane of focus. This is an exceptionally good way to visualize the *surface* of the cell about to be patch clamped, but it has perhaps an even greater virtue. Because of the very limited depth of field, it is possible to tell precisely when the electrode tip is located a very small distance above the cell surface. One focuses on the surface of the cell, defocuses to a position of a few micrometers above the cell, and then brings the electrode tip in focus by advancing the micromanipulator. This limits the distance over which high resolution but slow micromanipulator movements must be accomplished before the electrode makes mechanical contact with the cell surface. One is able to place the electrode tip onto the cell surface much more rapidly than with other optical principles. This technique is limited to use with inverted microscopes because of the Nomarski requirement for a relatively short objective working distance. To date, no one has implemented this technique with objectives that have the 10–20 mm working distances required for patch clamping with noninverted microscopes. Metallurgical microscopes with long working distance objectives can be used

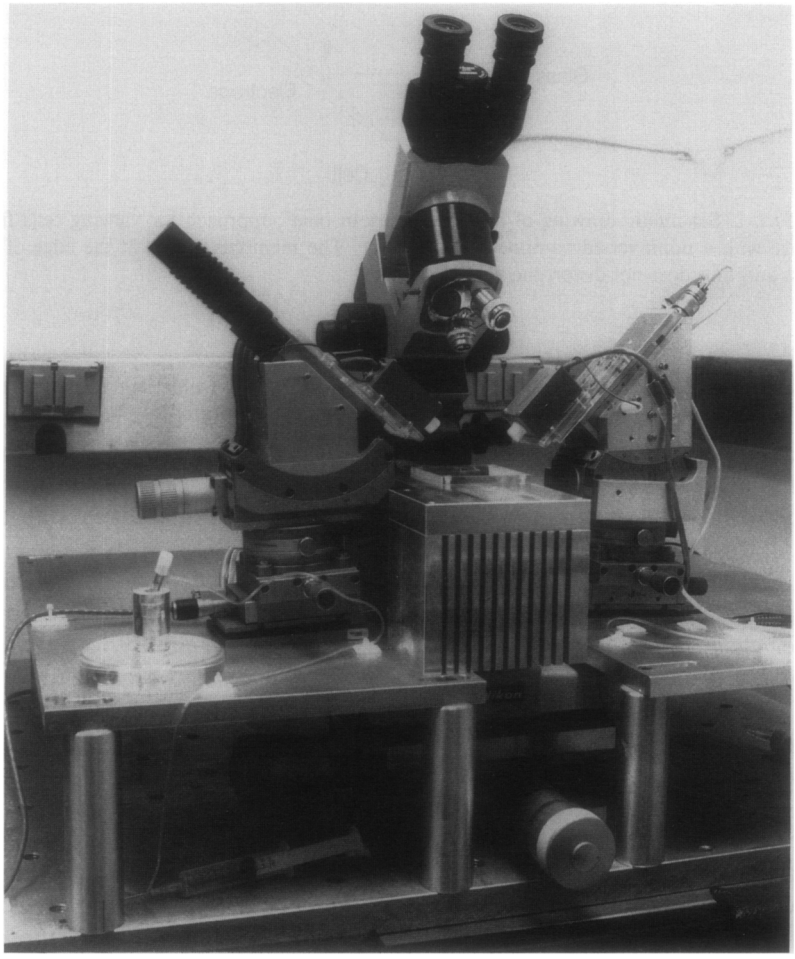

FIG. 3. An upright compound microscope with a hinge in its stand to allow the image-erecting binocular head to be folded back. (Such microscopes were first designed in the laboratory of R. S. Eisenberg at UCLA.) The manipulators shown have *x*, *y*, horizontal rotational, vertical rotational, and tilt motions. The headstage is mounted on a final motor drive.

with incident Nomarski interference contrast where delivery of light and viewing both occur through the objective. This has not proved effective with cells because of reflections from the surface of the bathing solution.

Many of the long working distance metallurgical objectives used with upright microscopes can be modified to implement the technique of Hoff-

man modulation contrast.[3] This optical approach produces a Nomarski-like image that also has a quite limited depth of focus. The optical slices produced, while still quite thin, are thicker than those possible with Nomarski optics in the inverted microscope. Much of this is dependent on the fact that the metallurgical objectives, for the same magnification, have smaller numerical apertures and therefore greater depth of focus than objectives with shorter working distances.

For one building a patch clamp setup on a limited budget, it is possible to implement a Schlieren microscopy principle as described by Axelrod.[4] This in general requires simply putting a piece of tape over about one-third to one-fourth of the back aperture of the objective and then placing an opaque object such as a black piece of paper between the light source and the bottom of the condenser. When this subcondenser "stop" is aligned parallel to the tape in the objective so as to yield a small slit for light passage, it is possible to get a Nomarski-like image, again with limited depth of field. Although this technique does not offer all of the resolution of Nomarski or Hoffman modulation contrast, it is often sufficient for patch clamping.

Another useful accessory for either an inverted or an upright microscope is a video camera and display. Inexpensive charge-coupled-device (CCD) cameras are most attractive for this purpose because of their small size. The major advantage of video viewing is that it allows the objectives to be used at their full numerical aperture. In general, high numerical aperture objectives produce rather weak contrast unless the iris diaphragm of the condenser is stopped down to a point where only 75 to 80% of the back aperture of the objective is filled with light. This arrangement produces contrast but at the loss of resolution. With a video-based system, the required contrast can be generated from the video electronics. This allows the iris diaphragm to be opened to a level that the back aperture of the objective is fully filled with light to provide the highest resolution. Although the cells will look very washed out through the eyepieces, even their internal structures will be exceptionally visible on the video monitor. One does have to be certain, however, that the video camera and its cables are sufficiently shielded that they do not provide electrical interference to the patch clamp recordings.

Micromanipulators

There is tremendous versatility in the micromanipulators that are available for patch clamping. Virtually every company that produces mechanooptical equipment and every microscope manufacturer sells a wide

[3] R. Hoffman and L. Gross, *Nature (London)* **254**, 586 (1975).
[4] D. Axelrod, *Cell Biophys.* **3**, 167 (1981).

variety of micromanipulators (see, for example, Newport, Founatin Valley, CA; Klinger Scientific, Garden City, NY; Daedal, Harrison City, PA; Pacer Scientific, Los Angeles, CA; Aerotech, Pittsburgh, PA). Many of these are probably perfectly adequate for patch clamp recordings. The main requirements are that the micromanipulators have a geometry that allows them to be located close to the preparation and that they be capable of repeatable movements of the order of one-tenth the diameter of the cells being studied. Also of extreme importance is that they not drift once the electrode tip has been placed in its desired final position. Obviously, it is desirable that they have mass, stability, minimum backlash, and be capable of repeatable submicron movements, but many investigators have used with good successs quite inexpensive micromanipulators which do not possess all of these characteristics.

Several features of micromanipulators are useful for the implementation of an optimal patch clamp setup. One is that they be capable of horizontal *angular* movement. If the manipulator has a horizontal rotation stage, it is possible to move the headstage very rapidly to a position where it is 45° to 90° lateral to its patch clamping position. This makes it possible to change rapidly the electrode holder and electrode, a need which on some days occurs all too often. A second desirable motion is angular movement along the vertical plane. This movement, often performed by a device called a goniometer cradle, allows one to move the electrode from a position above the bath downward to very near the cell surface in a minimum of time. The best goniometer cradles have both coarse and fine controls over this movement, allowing one to place the electrode tip to within a few microns of the cell surface easily and rapidly (see Fig. 3).

Many investigators have found it useful to have the final movement of the electrode tip onto the cell surface be under motor control. Most manufacturers of manipulators provide either stepping motor drives or dc-driven motors that are capable of producing movements of less than 1 μm per second. These devices provide optimal control in this critical step of pressing the electrode against the cell membrane. In some cases, this final movement is not motor driven but is driven from a very high resolution hydraulic system which can also yield very fine movements. Some manufacturers provide final movement via piezoelectric translators. This provides what is probably the finest control presently available. In the best of systems, it is possible to get x, y, and z movements all driven essentially simultaneously by a joystick mechanism that controls three piezoelectric translators. Joystick arrangements are also possible with hydraulic systems and with three-dimensional (3-D) motor drives. Such joystick-based systems are desirable but not necessary for a quality patch clamp setup.

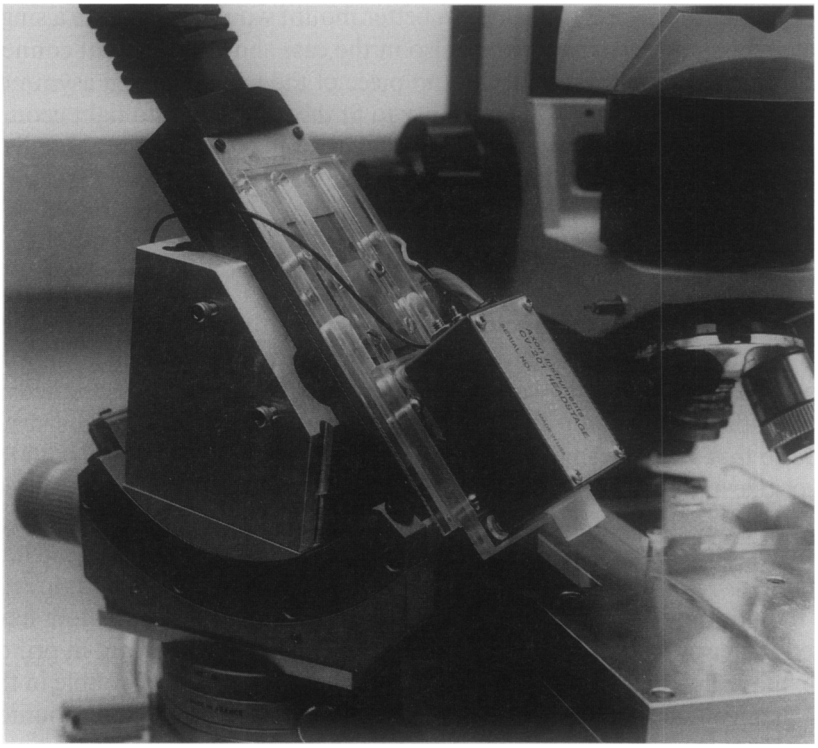

FIG. 4. Example of a method to mount a headstage to a final manipulator drive (see text).

Mounting the Headstage

In order for fine micromanipulators to do their jobs optimally, it is necessary that the patch clamp headstage be mounted on them in an optimal way and that the manipulators themselves be mounted on the rest of the setup in a way that their full potential is utilized. As a general principle, it is important that the headstage be rigidly attached to the micromanipulator. Some patch clamp companies provide their headstages with a long rod protruding from the back for mounting. With such a mount, it is possible for the headstage and the tip of the electrode to be suspended many inches from the center of mass of the micromanipulator. Although it is possible to do patch clamping under these circumstances, much better stability of the electrode tip is obtained if the body of the headstage is mounted to the manipulator via a rigid place. Figure 4 shows one such implementation. In this case the connection is made through a

pair of Plexiglas plates, but an even better mount would be through a single plate of a light but strong metal. Also in the case shown, the input connector is located in the center of the end piece of the headstage. An asymmetric location would improve the ability to fit the electrode into tight geometry like that under a long working distance objective or an intermediate working distance, higher numerical aperture condenser.

Mounting Micromanipulators

Again, as a general principle, it is important that the preparation and the micromanipulator be mounted in a way that movement between the electrode tip and the cell surface be minimized. This is best facilitated by having the manipulator and the preparation mounted on the same structure so that any movement of the structure simultaneously moves both the electrode and the cell. Three quite different approaches have been utilized. In the first, the preparation is mounted in a chamber attached to the movable stage of a microscope that focuses by moving the nosepiece. There the micromanipulator (usually a 3-D joystick variety) is mounted directly to the nonmovable part of the microscope stage. Many investigators have used such a system successfully even though the preparation can, in principle, move independently of the micromanipulators if there is wobble in the mechanical stage. Also, the kind of manipulators that can be mounted directly to the stage must be quite small and in general less able to support the weight of the headstage than can a more substantial micromanipulator.

A second way to mount manipulators is that chosen in the "patch clamp towers" (Fig. 5) (List Electronics, Eberstadt, Germany). Here, the entire preparation, microscope and all, sits on a metal plate to which an optical rail is attached rigidly. Optical rails come from almost any of the optical–mechanical supply houses (see, however, Klinger Scientific) and are designed, through commercially available mounts, to allow the attachment of a wide variety of mechanical components. In the best systems, an optical rail exists on each side of the microscope, and the tops of the two rails are firmly connected so as to provide exceptional stability. When these systems are used for patch clamp setups, one of the mechanical components is a very fine x–y stage suspended from the optical rail. This stage holds the chamber with the cells, takes the place of the microscope stage, and provides the source of x - y movement of the preparation. Attached to the same optical rail is the micromanipulator which can be quite simple or very complex depending on budget and inclination. Horizontal and vertical rotation as well as 3-D motor drive capability can be implemented on

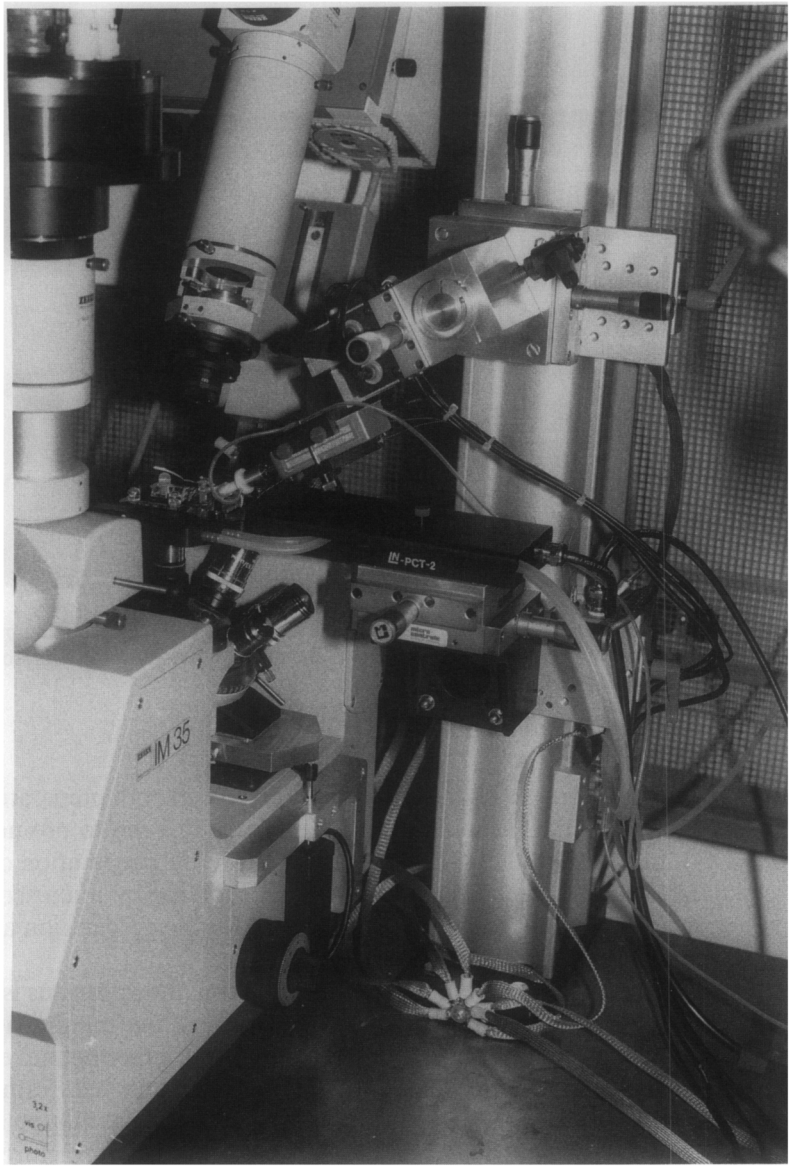

FIG. 5. Example of the patch clamp tower approach for mounting patch clamp hardware. Both the micromanipulator and specimen stage are connected to an optical rail. (Photo complements of Dr. J. Fernandez.)

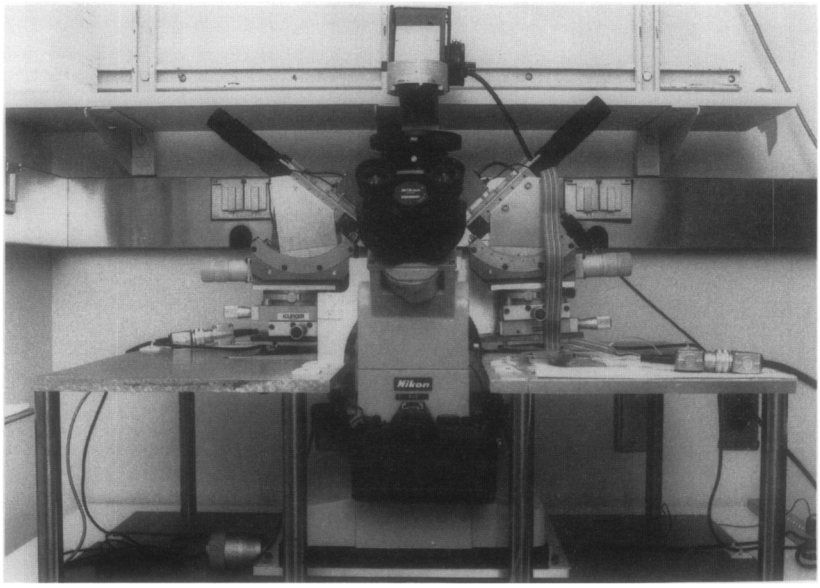

FIG. 6. Inverted microscope mounted on a movable $x-y$ table. The stage and manipulators are mounted to the metallic superstructure shown and do not move when the microscope is moved.

such systems. This is quite a favorable arrangement when both preparation and micromanipulators are mounted to the same optical rail to promote stability, but, in addition, the $x-y$ stages which move the preparation can be very much better than the mechanical stages supplied by microscope manufacturers. This results in a reduced tendency for the preparation and electrode to wobble with respect to each other.

At least potentially, the most rigid way of mounting the apparatus is to build a superstructure for holding the preparation and the manipulator very rigidly and then mount the microscope itself on a large toolmaker's $x-y$ stage. Under these circumstances, the cells are never moved. Rather, to find a new cell, the microscope is moved. One such implementation for an inverted microscope is shown in Fig. 6. When this superstructure is bolted to the tabletop, a very rigid structure is formed in which only the drift of the micromanipulator is important. In the other kind of mounts, drifts of the manipulators and the mechanical stages mounting the preparations are important.

It is not really known just how important the difference between these approaches is since all have been used successfully for patch and whole-cell

recordings. They are presented as simple guidelines to aid readers in the implementation of their personal setups.

Vibration Isolation

Because of the sensitivity of patch clamp recordings to even the slightest movements, it is necessary to mount the microscope, micromanipulators, and headstage electronics on a vibration isolation table. Buildings differ in the natural vibrations that they contain, but virtually all buildings have vibrations that come from slamming of doors, rotating electrical equipment, and many other sources. If these vibrations are not damped out, they will produce artifacts in the current recordings. The easiest solution is to mount the apparatus on an air suspension table of a variety that can be obtained from standard optical companies like Newport, Barry (Watertown, MA), and Micro-G (Peabody, MA). Such tables damp out vibrations that occur at frequencies beyond a few hertz. Unless building vibrations are particularly bad, air tables near the bottom of the line of these manufacturers are quite adequate. Vibrational components below a few hertz can be damped out only with either extremely massive tables (2000 lb tops or so) or with tables using active feedback. One problem with any kind of vibration isolation is that the apparatus used will have one or more resonant frequencies. This means that the devices may quite adequately reduce some vibrational components but they may actually enhance others which coincide with their resonant frequencies. Whereas this is usually not a problem with air suspension tables with heavy tops, it is quite common with homemade isolation devices in which metal plates are placed on top of tennis balls, foam rubber, Styrofoam padding, or a combination of several such materials. Although these home-grown vibration remedies often can be made to work very effectively, one must be certain that the various components used actually damp vibrations and not enhance them.

Shielding and Grounding

It is very important that the headstage, electrode, and preparation be adequately shielded from stray interference. Sixty-hertz frequency signals coming from line outlets, lights, or other electronic equipment are the most common contaminant of current recording records, but interference from antennas, computer screens, and other high frequency sources also occurs. Many investigators have chosen to surround their apparatus and vibration isolation equipment completely with a Faraday cage. It is, of course, important that the Faraday cage not actually touch the top of the vibration isolating apparatus. This cage is simply a conductive enclosure which

surrounds the preparation and is connected to ground. These enclosures interact with alternating electric fields to convert the signal to currents which are then shunted to ground through a low resistance connection.

The effectiveness of the shields depends on the frequency of the electric fields, being more effective for high frequency fluctuations than for low frequencies. Different materials have very different attenuation abilities for components of different frequencies. Copper and brass screening material which is commonly used for this purpose is less effective for 60-Hz signals than it is for high frequency signals. To attentuate 60 Hz substantially, the materials used for construction must provide electromagnetic shielding. Materials like mu metal are particularly good for this, although galvanized sheet metal and galvanized hardware cloth are also quite effective. In addition, there are new conductive plastic materials available that can be used. These plastic materials (like those used in shipping integrated circuits) can be obtained in large rolls and are particularly useful for constructing a drape at the front opening of the Faraday cage. This drape can be lifted out of the way while cells are being placed in the chamber, while the electrodes are being placed on the cells, etc., and then closed during recording. Many investigators have opted to make a Faraday cage of a good, solid electromagnetic shielding material on the top, back, and sides while utilizing a plastic drape in front. Another particularly useful feature of Faraday cages is that they can be built with small shelves on their internal walls which can be used for placing solution bottles, mounting pumps, or attaching other apparatus.

In many environments, Faraday cages are not required. Because patch clamp measurements are done in close proximity with either a microscope objective or a microscope condenser, excellent shielding can be achieved by simply grounding the microscope, the manipulator, and any conductive material in the region of the headstage, electrode, the cells. For this purpose, it is important that single-point grounding be used. The patch clamp headstage should have a high level signal ground point made available to the user. It is this point that must make low resistance contact with all of the conductive elements surrounding the cell chamber. If the setup is mounted on a metal frame and if the vibration isolation apparatus has a metallic top, these should also be connected to this ground through a resistance not to exceed 50Ω (ohms). It may be necessary to check all of the conductive elements around the setup with an ohmmeter to ensure that these low resistance contacts exist. Even if one uses a Faraday cage, this kind of single-point grounding should be used. In general, the Faraday cage is not connected to the high level signal ground but is connected to the instrument rack and/or to the ground terminal of a three-prong electrical plug.

Beyond these considerations, it is difficult to make general rules about grounding procedures. Because it is usually the case that one is trying to minimize 60-Hz interference, there are several approaches that one can use. To measure the impact of the procedures, connect the patch clamp current output to one input of the oscilloscope at sufficiently high gain that the 60-Hz signal largely fills the screen. The use of a 500-Hz bandwidth is good for this purpose. Couple via ac the input of the oscilloscope and synchronize the sweep to line so that the 60 Hz is synchronized with the screen sweep and appears not to shift in time. With proper grounding and shielding procedures, it should be possible to reduce the 60-Hz component so that it is somewhere between not detectable and 0.01 pA peak to peak. Quite often, it is adequate simply to plug the three-prong plug from each instrument into a grounded wall outlet, connect the structures on the vibration isolation setup to the single-point headstage ground, and connect the rack and Faraday cage to the ground pin of a three-prong outlet. If 60-Hz interference still remains, it is usually instructive to unplug one instrument at a time to locate one that is contributing 60 Hz. When such an instrument is found, it is common to reduce the interference by using a three-prong to two-prong adapter so as to isolate the ground of that particular instrument. If this approach does not work, it might be necessary to use three-prong to two-prong adapters on each of the power cords and then to test ways to ground each individual instrument to result in the lowest 60-Hz noise.

If problems persist, it can be useful to try to map the 60-Hz fields in the room where the apparatus is located. To do this, one can utilize a portable differential amplifier with a BNC cable extending from each of the inputs and with about 100 MΩ (megohms) of resistance connected between the two terminals at the opposite end of the cables. By connecting the amplifier output to the oscilloscope and by using the cables with the 100-MΩ resistor as an antenna, it is possible to probe various points in the room to identify sources of 60-Hz noise. When such sources are found, they can either be disconnected or somehow shielded so that their radiated 60 Hz is minimized. In most situations, one or more of the 60-Hz reducing procedures described here will be effective.

Major 60-Hz (or 120-Hz) interference may come from fluorescent room lights and from the microscope light itself. Often, the microscope light is driven by alternating current derived from the line and stepped down by a transformer in the microscope. Whereas in some cases it is possible to ground the microscope and the power cord to the light to adequately shield against this problem, more often one must rewire the microscope so that the light can be driven from a low ripple direct current power supply. Fluorescent lights in the ceiling over the preparation do not

cause much interference in Faraday cage-based facilities but may if shielding comes from simply grounding the microscope and its surroundings. In this case, it is necessary to work with the room lights turned off or to have the room light switch rewired so that the lights specifically above the setup can be turned out. Some investigators have even installed dimmable incandescent lights near their setups since these do not produce the large fields that fluorescent lights do.

Patch Clamp Electronics

High quality patch voltage clamps are available from several manufacturers. Although most of these instruments have many features in common, some are exceptional in particular areas. Rather than describe the various features of patch clamps from specific manufacturers, we will here discuss some theoretical and practical aspects of patch clamp electronics in its present state of the art, leaving the choice of particular instruments to the reader. Our discussion will emphasize the patch clamp headstage, that is, the current to voltage converter which measures the patch and whole-cell currents, since in many respects this is the most critical portion of the overall electronics.

Headstage

There are two basic varieties of patch clamp headstages which we will denote as resistive feedback headstages and capacitive feedback headstages. Some manufacturers provide both resistive feedback and capacitive feedback in a single switchable headstage design; in this case the capacitive feedback mode is generally intended for ultra-low noise measurements of single channels, and the resistive feedback mode is intended for whole-cell voltage clamping.

Resistive Feedback Headstages. The resistive feedback circuit is well known, and its basic characteristics have been described in detail elsewhere.[1,5] Fundamentally, the circuit uses negative feedback from the output of the operational amplifier to its inverting input to maintain this input at a "virtual ground." The current source being measured, i, is attached to the inverting input. The JFET (junction field-effect transistor) input of the operational amplifier draws essentially no current (<1 pA dc) at its gate (i.e., the inverting input) so that current entering this node is forced to flow through the feedback resistor, R_f. The amplifier output develops a voltage,

[5] F. J. Sigworth, *in* "Single-Channel Recording" (B. Sakmann and E. Neher, eds.), p. 3. Plenum, New York and London, 1983.

V_o, which is proportional to the input current, that is, $V_o = -iR_f$. When used in a patch voltage clamp, the patch pipette is attached to the inverting (−) input of the operational amplifier, and the circuit is modified so that command voltages, V_c, are applied to the noninverting (+) input; as a result of feedback the command voltage will also be imposed on the inverting input, that is, at the top of the patch pipette. It should be noted that most commercial patch clamps utilize a discrete JFET input stage in conjunction with a commercial operational amplifier to create the headstage amplifier. This approach leads to lower noise than is possible by using any operational amplifier that is presently commercially available. Details of such designs have been presented elsewhere.[1,5]

Because the currents that are measured with a patch voltage clamp are so small, an extremely high valued feedback resistor is used both to provide adequate gain and to achieve a good signal-to-noise ratio (the input referred current noise of the feedback resistor is inversely proportional to the square root of its value). For single-channel measurements, the value of R_f is typically 50 GΩ; for whole-cell current measurements, 500 MΩ to 1 GΩ is typical in most commercial instruments. Most of the shortcomings of resistive feedback headstages arise from nonideal characteristics of these high valued resistors.

The power spectral density of the thermal current noise of an ideal feedback resistor, R_f, is given by $4kT/R_f$, where k is Boltzmann's constant and T is the absolute temperature. The root mean square (rms) noise in a given bandwidth, B, is given by $[(4kT/R_f)B]^{1/2}$. From these relationships, it is obvious that larger valued feedback resistors will produce less noise. However, all commercially available gigohm-range resistors with which we are familiar exhibit considerable amounts of noise in excess of the expected thermally induced noise fluctuations. Excess noise occurs at both low frequencies and high frequencies. Low frequency excess noise has the familiar $1/f$ spectral form; its amplitude is quite variable even among feedback resistors of the same type. $1/f$ noise is not a particularly important problem for patch clamp measurements, although it can place limits on the background noise when very small bandwidths are used. Excess high frequency noise in gigohm feedback resistors is a much more severe problem for patch clamp measurements. All commercially available gigohm-range feedback resistors have noise spectral densities which rise above the expected thermal noise level beginning at frequencies that range from a few hundred hertz to a few kilohertz. Even with the best resistors that we know of, this excess noise can account for about half the total noise of the headstage at a bandwidth of 10 kHz. For poorer resistors, high frequency excess noise can be the dominant noise source at all bandwidths above a few kilohertz.

Another drawback to using gigohm-range feedback resistors is the small bandwidth of the current signal directly at the headstage output. The frequency response of a resistive feedback headstage is limited by the stray capacitance, C_f, shunting the feedback resistor. For example, 0.1 pF of stray capacitance associated with a 50-GΩ resistor will lead to a time constant of 5 msec which corresponds to a bandwidth (−3 dB, one-pole RC filter) of only 32 Hz. Because this bandwidth is inadequante for almost all patch clamp measurements, a "boost" circuit is required to restore the high frequency components of the signal and, of course, of the background noise. It can easily be shown[1,6] that the effective band width can be increased by this circuit from B_{HS} (the headstage bandwidth, $B_{HS} = 1/(2\pi R_f C_f)$ to approximately $(B_{HS}B_u)^{1/2}$, where B_u is open loop unity gain bandwidth of the operational amplifier used in the boost circuit. For example, for $B_{HS} = 80$ Hz (time constant ~2 msec) and $B_u = 20$ MHz, a final "boosted" bandwidth as high as 40 kHz can be achieved. It should be noted, however, that the response will no longer be first order. Obviously, the final bandwidth can be larger for relatively small feedback resistors (e.g., 50–500 MΩ) than for very high valued resistors (e.g., 50 GΩ). Reducing the stray capacitance that shunts the feedback resistor could also increase the intrinsic headstage bandwidth (B_{HS}), although a low value of this capacitance can have adverse effects when the headstage has a large capacitive load at its imput.[7]

In addition to the inherently limited bandwidth associated with gigohm-range resistors, it is also important to realize that the conductive path of most or all such resistors is nonuniform, so that the stray capacitance is distributed and the frequency response can be quite complex. This necessitates the use of two or more stages of boost circuitry to produce an adequately flat high frequency response. Such circuitry not only further restricts the final boosted bandwidth, but also provides more possible locations for drift with time and temperature which can slightly "detune" the boosted response. Finally, nonlinearities (see below) associated with high valued feedback resistors can somewhat change the shape of the boosted response as a function of signal level.

Three other limitations of high valued feedback resistors should also be noted: (1) relatively large voltage coefficients of resistance, (2) large temperature coefficients of resistance, and (3) rather poor stability with time (aging). The voltage coefficient of resistance of commercially available

[6] R. Levis, "Patch and Axial Wire Voltage Clamp Techniques and Impedance Measurements of Cardia Purkinje Fibers." University Microfilms International, Michigan and London, 1981.

[7] W. D. Niles, R. A. Levis, and F. S. Cohen, *Biophys. J.* **53**, 327 (1988).

gigohm resistors can be as high as 4–6% per volt which would mean that the resistance value would change by 40–60% as the headstage output swings from 0 to 10 V. Obviously, so great a nonlinearity is unacceptable for most patch clamp work. The chip resistors used by several commercial patch clamp manufacturers are substantially superior to this, but their voltage coefficients are not small enough to be ignored. In fact, the voltage coefficient of these resistors is itself nonlinear, varying from as much as 1% per volt for small fields (≤ 1 V) to less than 0.5% per volt for voltages in the vicinity of 10 V. Typical values are somewhat better, and lower value resistors (e.g., 500 MΩ) usually outperform higher value resistors (e.g., 50 GΩ). For the measurement of single-channel currents or of most whole-cell ionic currents, these nonlinearities are usually acceptable. However, when procedures like $P/4$ pulse protocols are used to eliminate linear capacity transients (e.g., for measurements of "gating" currents from whole cells[8]), such nonlinearities can become quite important, and it is necessary to use capacity and whole-cell compensation (see below) to eliminate as much of the linear transient as possible in order to minimize the output voltage excursions of the headstage. These nonlinearities can also lead to minor differences in the adequacy of the boost circuitry for signals of different amplitude.

The temperature coefficient of resistance (TCR) of all gigohm-range resistors is substantially higher than those of precision resistors with values less than about 100 MΩ. Such coefficients generally fall in the range of 0.1–0.5%/°; 0.2%/° is more or less typical. These values indicate that gain changes of as much 1% can occur with normal temperature variations in laboratory environments. Perhaps more importantly, it should be realized that during the first 30 min or so after the instrument is turned on, resistance values will slightly change as the headstage warms up. Some manufacturers have chosen to heat the feedback resistor (as well as nearby components) to a stable value above the normal range of room temperatures. This greatly reduces temperature-induced drift, but comes at the expense of greater gate current for the input JFET and increased low frequency noise.

Gigohm resistors are also generally less stable with time than lower valued precision resistors. Resistance changes of 2–5% per year are possible. Because of this it is a good idea to periodically (every 6 months or so) calibrate the gain of the patch clamp and, since resistance changes can effect the "tune" of the boosted response, check the performance of the boosted output at the same time.

[8] B. P. Bean and E. Rios, *J. Gen Physiol.* **94,** 65 (1989).

Despite the numerous shortcomings of high valued feedback resistors, resistive feedback headstages are quite adequate for most patch clamp measurements and, of course, have been used successfully for many years. In general, resistive feedback is still the only real option for whole-cell recording. However, recent advances in patch clamp technology have provided the user with a very effective alternative for single-channel measurements. This is the capacitive feedback (integrating) headstage. In the future, such headstage designs may also become more practical for whole-cell measurements.

Capacitive Feedback Headstages. Compared to highly imperfect gigohm-range feedback resistors, small capacitors are nearly ideal circuit elements. Small ceramic chip capacitors can have leakage resistances as high 10^{15} Ω. Such capacitors are almost perfectly linear over the typical range of voltages encountered in patch clamp instrumentation (±10–15 V), and their frequency response is ideal to well beyond 1 MHz. Of even greater importance is the fact that capacitors introduce essentially no thermal or excess noise of the type described above for gigohm resistors. Because of this, the noise of a capacitive feedback headstage can be substantially lower than that which can be achieved with any resistive feedback element. Capacitive feedback headstages also offer wider bandwidth (with a perfectly flat transfer function up to the high frequency cutoff) and greatly extended dynamic range when compared to resistive feedback. The only major drawback of the new technology is the necessity to reset periodically the headstage output to zero; a lesser difficulty arises from dielectric absorption. These subjects are discussed below.

The current-to-voltage converter consists of an operational integrator followed by a differentiator. It is easily shown that the gain, R_g (ohms), of the integrator/differentiator combination is given by

$$R_g = R_d(C_d/C_{fi})$$

that is, $V_{od} = iR_d(C_d/C_{fi})$, where V_{od} is the output of the differentiator, C_{fi} is the feedback capacitor of the integrator, C_d is the input capacitor of the differentiator, and R_d is the feedback resistor of the differentiator. Typical values would be $C_{fi} = 1$ pF, $C_i = 10{,}000$ pF, and $R_d = 100$ kΩ, providing a current-to-voltage gain of 1 GΩ. As described below, the noise of the capacitive feedback headstage can be made to be essentially independent of its gain. This is very different from the situation with resistive feedback where gain and noise are intimately linked, that is, low noise requires a high valued feedback resistor.

The bandwidth of a capacitive feedback headstage can be very large relative to that which can be achieved using resistive feedback. The achievable bandwidth (or natural frequency, f_N) of the integrator/differentiator

combination is well approximated in terms of the gain R_g ($R_g = C_d R_d / C_{fi}$), the feedback capacitance, C_{fi}, and the open loop unity gain frequency of the differentiator, f_{ud}, that is,

$$f_N = 1/[2\pi R_g (C_{fi}/f_{ud})]^{1/2}$$

For $R_g = 1$ GΩ, $C_{fi} = 1$ pF, and $f_{ud} = 80$ MHz, this indicates that a bandwidth of 110 kHz can be achieved; by reducing the gain to 100 MΩ the bandwidth can be extended to about 350 kHz. Clearly, wide bandwidth is associated with a fast differentiator amplifier, small values of C_{fi}, and low values of gain, R_g. Recall, however, that for the capacitive feedback headstage, low noise can be achieved even for low values of R_g.

The very wide bandwidth possible with capacitive feedback may well prove to be important in the future, but it should be noted that, at the present time, bandwidths of more than about 20 kHz are of questionable value to patch clamping or whole-cell measurements using the patch voltage clamp. This is because the noise of either resistive or capacitive feedback headstages increases steeply with increasing bandwidth, ultimately increasing as the bandwidth to the 3/2 power. The lowest noise we have achieved to date in an actual patch recording situation is about 0.25 pA rms (about 1.5 pA peak to peak) in a 10-kHz bandwidth. For a 20-kHz bandwidth, this should increase to about 0.7 pA rms (about 4.2 pA peak to peak), and for a 50-kHz bandwidth it should reach about 2.8 pA rms (about 17 pA peak to peak). Obviously even under ideal circumstances, such large bandwidths could only be used with extremely large single-channel currents. In the case of whole-cell clamping through a patch pipette, the actual bandwidth of current recording in the absence of series resistance compensation is limited to $1/(2\pi R_s C_m)$, where R_s is the series (pipette) resistance and C_m is the membrane capacitance. For $R_s = 10$ MΩ and $C_m = 50$ pF, this amounts to only about 320 Hz. A much larger recording bandwidth would only add noise to the measurement, not more information about the current signal. If series resistance compensation is used, then the actual bandwidth of current measurement will be $1/2\pi R_{sr} C_m$, where R_{sr} is the residual (uncompensated) series resistance (e.g., for $R_s = 10$ MΩ and 90% compensation, $R_{sr} = 1$ MΩ). In the previous example, 98.4% compensation would be required to justify a 20-kHz bandwidth. At this bandwidth (with $R_s = 10$ MΩ and $C_m = 50$ pF), the noise in the measurement would be more than 250 pA rms (1.5 nA peak to peak).

The noise of a capacitive feedback headstage can be substantially lower than that of a resistive feedback headstage. The reason for this is primarily due to the thermal and excess high frequency noise associated with gig-

ohm-range resistors. At low to moderate frequencies, the floor of the resistive feedback headstage noise power spectral density is determined primarily by the thermal noise of the feedback resistor; with good input field-effect transistors (FETs) the input current noise associated with FET gate leakage current, i_g, is of lesser importance. In the capacitive feedback headstage, the low frequency noise floor is determined almost exclusively by the current noise of the FET gate current. For FETs that are also good selections for low noise at high frequencies, i_g can be as low as 0.1 pA or somewhat less, and the power spectral density of the input referred noise at low frequencies can be 10 times lower than that which is achieved with a 50-GΩ resistor. Thus, at low frequencies, the noise performance of the capacitive feedback headstage is definitely superior to that of a resistive feedback headstage. At higher frequencies, the noise of the capacitive feedback headstage is dominated by the input voltage noise of the FET input, which in conjunction with the input and stray capacitance at the input (plus the small feedback capacitor) produces current noise with a power spectral density that rises as frequency squared. This same noise source is present in resistive feedback headstages, but, as described above, excess high frequency noise from the feedback resistor typically produces as much or more noise at high frequencies.

Of course, real capacitors are not completely free of noise; some dielectric noise (see discussion below) will be present, but with high quality capacitors (dissipation factor less than 0.0001) dielectric noise of the feedback and compensation capacitors will be negligible by comparison with other noise sources. Noise associated with the differentiator can be made negligible by careful circuit design. In particular, noise associated with the differentiator is minimized by selecting a low-noise FET input operational amplifier (e.g., Burr-Brown, Tucson, AZ; OPA 101/102 or OPA 627) for this location and by keeping the ratio C_d/C_{fi} large.

On the basis of the above discussion it would be predicted that a capacitive feedback headstage could be built utilizing a differential U430 JFET (Siliconix, Santa Clara, CA) input stage with noise in the range of 0.12–0.15 pA rms in a 10-kHz bandwidth; this can be compared with 0.25–0.3 pA rms for high quality resistive feedback headstages. In actual practice, the noise of practical capacitive feedback headstages is found to be somewhat higher, typically in the range of 0.18–0.20 pA rms in a dc 10-kHz bandwidth (−3 dB, 8-pole Bessel filter). There are several reasons for this. One additional noise source arises from the switch used to reset the headstage periodically. In addition, compensation signals used to balance currents injected by this switch during and just following reset and to eliminate the effects of dielectric absorption of the feedback capacitor inevitably add small amounts of noise. A certain amount of noise must

also be expected to result from the packaging of critical components of the input stage and from the input connector. This noise results both from the addition of stray capacitance at the input and from dielectric noise (see discussion under electrode noise below) associated with the packaging and connector. Nevertheless, capacitive feedback can produce significantly lower noise patch clamp measurements than could previously be achieved using resistive feedback. We have achieved noise as low as 0.13 pA rms in a 5-kHz bandwidth in actual patch recording situations using capacitive feedback headstages, whereas with resistive feedback it is generally rare to go below 0.20 pA rms in the same bandwidth. Of course, to achieve these results it is essential to minimize all other sources of noise as described elsewhere in this chapter (see also [3] in this volume).

Further improvements in the noise of capacitive feedback headstages can be anticipated. It seems possible that headstage noise as low as 0.06–0.10 pA rms in a 10-kHz bandwidth can be achieved. Approaches to produce such noise reduction are not discussed here, but we believe that such low levels of headstage noise can be of practical significance to overall noise performance. The present and predicted limits of noise performance in patch voltage clamping are discussed below.

The dynamic range of a capacitive feedback headstage can also greatly exceed that of resistive feedback devices produced for low-noise measurements. The reason for this is basically the fact that with capacitive feedback gain and noise are not linked as they are in a resistive feedback headstage. Because the feedback capacitor lacks the thermal and excess noise associated with feedback resistors and because the noise contribution of the differentiator can be made negligible, it is possible to produce a capacitive feedback headstage with a gain of 100 μV/pA and input referred noise of less than 0.2 pA rms in a 10-kHz bandwidth. Even lower gains can be produced with the same input referred noise, although numerous precautions must be taken to ensure that noise of subsequent stages of the electronics (gain, filters, etc.) do not elevate the intrinsic headstage noise in such cases. To achieve noise in the range of 0.25–0.30 pA rms in a 10-kHz bandwidth with resistive feedback it is traditional to use a 50-GΩ resistor resulting in a minimum gain of 50 mV/pA. Thus, the dynamic range (defined, e.g., as the ratio of the full scale output to the minimum detectable signal) of the capacitive feedback headstage can be 500–1000 times larger than is possible with a 50-GΩ resistive feedback headstage. Of course for many measurements an output gain of 100 μV/pA may be undesirably small, particularly when the sensitivity of the final analog-to-digital converter is considered. In this situation it is only required that gain be provided following the integrator/differentiator.

At the present time, the very large dynamic range available with capac-

itive feedback has relatively limited utility for most biophysical measurements, but we feel that its existence will become more useful in the future. Additional benefits associated with capacitive feedback as compared to resistive feedback are (1) improved fidelity of current measurement, (2) improved linearity, (3) very low temperature coefficient of gain, and (4) the ability to pass very large transient currents.

As described in the previous section, resistive feedback headstages often require rather complicated high frequency "boost" circuitry to deal with the limited and somewhat complex frequency response of high valued feedback resistors. Even with such circuitry, aberrations of the step response with amplitudes as large as 2–3% of the total and durations as long as several milliseconds are sometimes unavoidable; the nature of these distortions can also vary somewhat as a function of signal level. The integrator/differentiator combination of capacitive feedback is completely free of such distortions.

In addition, the small feedback capacitor of the capacitive feedback headstage is almost perfectly linear over the range of voltages (± 10 V) encountered. The differentiator can also be easily made to be highly linear. This is a distinct improvement over the situation described above for most high valued feedback resistors. This capability for highly linear operation suggests to us that capacitive feedback may become useful in whole-cell recording as well as single-channel measurements. Improved linearity can be quite important in measurements such as whole-cell gating currents which rely on the subtraction of relatively large currents to reveal to smaller signal of interest. To be practical for most whole-cell measurements the size of the feedback capacitor should be increased (e.g., to 10 or 20 pF) to reduce the frequency of occurrence of resets.

The temperature coefficient *(TC)* of the gain of the capacitive feedback headstage can also be significantly less than that of resistive feedback. The *TC* of small ceramic chip capacitors suitable for use as the feedback element in the integrator is typically about 70–90 ppm/° (as compared to 2000 ppm/° for typical gigohm feedback resistors). By matching the *TC* of the input capacitor of the differentiator to that of the integrator (and using a low TCR resistors in the differentiator and subsequent electronics, which are readily available for resistors with values less than 1 MΩ) it should be possible to reduce the overall *TC* to about 10–20 ppm/°.

A capacitive feedback headstage can also readily supply large transient currents required to charge capacitive loads quickly without saturating the integrator. With a 1-pF feedback capacitor and a 10-V output voltage, 10 pC of charge (e.g., 1 nA for 10 μsec or 10 nA for 1 μsec) can be applied without saturation (or reset). With a 50-GΩ resistor and a 10-V output, the maximum current that can be passed is 200 pA. Of course the transient

current passing ability of a resistive feedback headstage can be increased by placing a capacitor in parallel with the feedback resistor, but this is generally only practical for small (e.g., 500 MΩ) feedback resistors since with very large resistors the reduction of the intrinsic headstage bandwidth would be too great.

The only drawback to the capacitive feedback headstage is the necessity to reset periodically (i.e., discharge) the integrator feedback capacitor. The dc component of the current being measured, i, plus the gate leakage current, i_g, of the input FET will drive the output voltage of the integrator, V_{oi}, toward saturation at a rate given by

$$dV_{oi}/dt = (i + i_g)/C_{fi}$$

For $C_{fi} = 1$ pF and $i_g = 0.1$ pA, the output of the integrator will ramp upward at a rate of 100 mV/sec even in the absence of any measured current; saturation (about 10 V) would be reached in about 100 sec. Obviously, measured currents will drive the output toward saturation more quickly: a total average current of 10 pA (e.g., a 20-pA channel that is open half of the time or 100 mV across a 10-GΩ seal) would cause the output to reach 10 V in 1 sec, 100 pA of dc current would cut this time to 100 msec.

The solution to this problem is to discharge the integrator capacitor rapidly and thereby reset the output voltage of the integrator to zero. Of course during the period of time that the feedback capacitor is shorted, the current at the input of the headstage will not be measured. It is therefore important to keep the duration of reset as short as possible. It is not dificult to reset the integrator capacitor in 5–10 μsec. On the other hand, resetting the differentiator capacitor is somewhat more difficult. This is both because the differentiator input capacitor is much larger than the integrator feedback capacitor and because even if the differentiator capacitor itself is discharged in a few microseconds, transients associated with this reset as they appear at the differentiator output will have a duration that is in part determined by the bandwidth of the integrator/differentiator combination. For example, for a bandwidth at the differentiator output of 100 kHz something of the order of 20 μsec following the *end* of the actual reset (shorting) period is required for the transient to settle back into the noise. Because the measured output is replaced by the output of a modified sample and hold circuit as long as the actual output is perturbed by the reset transient, the need for a wide bandwidth at the differentiator output is dictated more by the requirement of keeping the total reset time (i.e., the time that the output does not accurately reflect the input current) as brief as possible than by the present usefulness of such wide bandwidths to biophysical measurements.

The total duration of the reset is typically some 30–50 μsec. During

this period the output does not accurately reflect the input current. When the output is filtered with a cutoff frequency in the neighborhood of 5 kHz or less resets can be essentially undetectable, provided that dielectric absorption effects have been adequately canceled. Even so, data obtained during the brief reset period are not valid, and for this reason manufacturers of capacitive feedback headstages typically provide a "telegraph" signal indicating the occurrence of a reset. For pulsed data acquisition (e.g., as is typical for the measurement of voltage-gated ionic channels) resets can generally be avoided during the period in which data are recorded by forcing a reset just prior to the step voltage command.

Other Aspects of Patch Clamp Electronics

Aside from the type and quality of the headstage, there are a variety of other features that are important in patch clamp electronics. Many such features only provide added convenience, whereas others may be essential in various situations. We very briefly describe a few such features here.

Capacity Compensation. Stray capacitance at the headstage input plus the capacitance of the holder and pipette must be charged with the pipette potential is changed. As described in [3], this volume, the pipette capacity transient has a large fast component plus a smaller slower tail arising from the lossy dielectric characteristics of the glass. For resistive feedback headstages with R_f values of 50 GΩ even relatively small voltage steps can result in saturation of the headstage output during the charging of the fast capacity transient; for a 100-mV step, saturation will typically persist for 1 msec or more. Obviously single-channel data are lost during this period. The solution is to inject the charging current by a separate pathway, usually a 1-pF capacitor internally connected to the input. For capacitive feedback headstages, saturation is unlikely to occur, and so fast capacity compensation, although still desirable, is not as necessary. Essentially all commercial patch clamps provide fast capacity compensation. Some manufacturers also provide a slower component to help to cancel the tail of capacity current resulting from the pipette. Because the slow component arising from the pipette is not well described by a single exponential (see [3] in this volume), the cancellation provided is not perfect. For both slow and fast components of capacity compensation it is important for low-noise measurements that the compensation circuitry not add a significant amount of noise above that of the headstage alone.

Whole-Cell Compensation. It is often useful to cancel the current involved in charging the cell membrane capacitance during whole-cell recording. Several commercial patch clamps provide circuitry to accomplish

this. It is important to realize, however, that by itself such compensation does nothing to speed the response time of the cell potential which is determined by the time constant R_sC_m. Some form of "supercharging" can speed up the membrane potential response but will not reduce membrane potential errors resulting from the flow of ionic current. Series resistance compensation will both speed up the membrane potential response and reduce errors arising from ionic currents. Whole-cell capacity compensation is usually designed so that the transient will continue to be appropriately canceled as series resistance compensation is advanced. The effects of series resistance on whole-cell voltage clamping are considered in greater detail below.

Compensation for whole-cell capacity transients can be particularly important when a *"P/N"* (e.g., the traditional *P*/4) procedure is used, for example, to study gating currents from whole cells. Nonlinearities of the feedback resistor (especially its voltage coefficient of resistance) can produce substantial artifacts in such situations unless the cell membrane capacity transient has been adequately reduced in size (i.e., canceled) so that the output excursions of the headstage remain relatively small.

Other features of patch clamp electronics, such as pipette offset, "tracking," current clamp, output gain stages, and filters, are not discussed here. The importance and use of such features are well explained in the manuals provided with commercial patch voltage clamps.

Noise Considerations for Patch Clamp Recording

Electrode Noise

In addition to the inevitable noise arising from the membrane–glass seal (see section on seal noise below), the pipette contributes noise to the measured current in patch voltage clamping by several mechanisms. In the first place, the holder and pipette are major sources of capacitance at the headstage input and will therefore react with the input voltage noise, e_n of the headstage to produce current noise with a power spectral density (PSD, A^2/Hz) that will rise as f^2 at frequencies above which e_n has become essentially constant (typically ≥ 1 kHz). This noise is perfectly correlated with the noise arising from the intrinsic capacitance, C_{in}, associated with the gate input of the JFET input stage of the headstage and its input voltage noise, and therefore the usual rules of root mean square noise addition do not apply. It should be noted that C_{in} consists of the JFET input capacitance ($C_{iss} = C_{gs} + C_{gd}$, where C_{gs} is the gate to source capacitance and C_{gd} is the gate–drain capacitance) plus 1–2 pF of stray capacitance, plus the

capacitance of the injection capacitor connected to the gate for compensation signals (typically 1 pF), and, for a capacitive feedback headstage, the feedback capacitor, C_{fi} (1–2 pF). If the holder plus pipette capacitance is denoted by C_{hp}, then the noise PSD associated with E_n will be given by $4\pi^2 e_n^2 (C_{in} + C_{hp})^2 f^2$. In general, e_n will be a function of frequency with $1/f$ noise dominating at low frequencies (< 100–1000 Hz for good JFETs) and a limiting high frequency value; it is often adequate to approximate e_n^2 by its high frequency limit when relatively wide bandwidth (say > 2–3 kHz) noise is considered.

The capacitance of the holder can range from about 1 to 5 pF depending on construction and the presence of absence of metallic shielding (which increases capacitance); the holders we use are unshielded and, by themselves, add only about 1–1.5 pF. The capacitance added by the pipette depends on a variety of factors including the depth of immersion of the pipette into the bath, the type of glass used, the ratio of outer to inner diameter, and the use of Sylgard coating. For uncoated pipettes, pipette capacitance ranges from about 0.5 to somewhat more than 2 pF per millimeter of immersion (see below). Sylgard coating can, however, significantly reduce these values. In general the total capacitance from the pipette alone will typically fall in the range of 1–5 pF. Thus, C_{hp} should range from about 2 to 10 pF. For well-designed differential headstages that are presently available e_n is generally in the range of 1.5–3 nV/Hz$^{1/2}$ ($f \geq 1$ kHz). C_{in} is typically about 15 pF. Assuming that e_n is 2 nV/Hz$^{1/2}$ and C_{in} is 15 pF, then in a 10-kHz bandwidth (−3 dB of an 8-pole Bessel filter) e_n–C_{in} noise will amount to about 0.15 pA rms. For C_{hp} equals 2 pF, the total noise arising from e_n would increase to 0.17 pA rms again for a 10-kHz bandwidth; for C_{hp} equals 10 pF this value would increase to 0.25 pA rms. Obviously, in terms of noise it is important to keep C_{hp} as low as possible.

It should also be obvious that if headstages become available with smaller values of e_n (without significantly increasing C_{in}), both the noise of the open-circuit headstage and the noise increment associated with C_{hp} will decrease; for example, for $e_n = 1$ nV/Hz$^{1/2}$ and the same C_{in} all of the root mean square values presented above would be cut in half. From the point of view of headstage design, the selection of the best JFET for the input stage should be based on the product of e_n and the total noise producing capacitance, C_T ($C_T = C_{in} + C_{hp}$), associated with it in an actual measurement situation. It can easily be seen that headstage amplifiers could be produced with essentially identical open-circuit noise which would behave differently when loaded with capacitance at the input. For example, a headstage with $e_n = 6$ nV/Hz$^{1/2}$ and $C_{in} = 5$ pF would produce the same

$e_n - C_{in}$ noise (and presumably the same total open-circuit headstage noise) as a headstage with $e_n = 1.2$ nV/Hz$^{1/2}$ and $C_{in} = 25$ pF; in a 10-kHz bandwidth (8-pole Bessel filter) e_n would be responsible for about 0.15 pA rms in each case. However, with $C_{hp} = 5$ pF, so that C_T is 10 pF for the first amplifier and 30 pF for the second amplifier, the "$e_n - C_T$" would be 0.30 pA rms in the same 10-kHz bandwidth for the amplifier with $e_n = 6$ nV/Hz$^{1/2}$ but only 0.18 pA rms for the amplifier with $e_n = 1.2$ nV/Hz$^{1/2}$.

A useful figure of merit for FETs is the ratio of their transconductance, g_m (mhos), to C_{iss}. The transconductance is approximately related to the input voltage noise (beyond the 1/f region) by $e_n^2 \cong 4kTv/g_m$, where v is theoretically equal to 0.67, but is usually higher. For the lowest noise this ratio should be as large as possible; for the best JFETs presently available, $g_m/C_{iss} \cong 1.0 - 1.5 \times 10^9$ sec^{-1}. Ratios about this good are, however, available from several different JFETs, some with relatively small g_m (and therefore relatively high e_n) and small C_{iss} and others with high g_m and C_{iss}. If g_m/C_{iss} were identical for all such FETs then the best selection would be a FET with C_{iss} approximately equal to the sum of the holder and pipette capacitance plus any compensation capacitors connected to the input, plus, for capacitive feedback headstages, the feedback capacitor, plus any stray capacitance at the input; this capacitance should total roughly 5 - 10 pF. However, unless the FET is cooled, the value of input gate current, i_g, must also be taken into account; some JFETs with very low e_n have rather high values of i_g and are thus impractical for patch clamp devices. In addition, some JFETs have higher values of e_n than would be predicted from their transconductance. It also seems likely that the choice of an optimum value of C_{iss} could be effected in a frequency dependent manner by the dielectric noise of the silicon itself. Of JFETs that are commercially available at the time of this writing, the U430 still is an excellent selection for the input stage of the patch clamp headstage. Nevertheless, improvements should be possible. In principle g_m/C_{iss} is linearly related to the carrier mobility of the material used to fabricate the FET; thus gallium arsenide FETs would be expected to have substantially lower e_n for a given value of C_{iss} than silicon FETs. This is in fact true at very high frequencies; however, at the present time all such FETs that we know of have very large amounts of $1/f$ noise which extends beyond the uppermost frequency used in patch clamping.

Short channel JFETs should also be attractive; g_m/C_{iss} theoretically varies as $1/L^2$, where L is the FET channel length. In most commercially available JFETs L is not less than roughly 10 μm, but it should be possible to significantly reduce this without too greatly increasing i_g. This suggests the possibility of producing silicon JFETs with g_m/C_{iss} ratios as high as

$3-5 \times 10^9$ sec^{-1}. Such a FET, with C_{iss} of 3–10 pF, if it becomes available, would be ideal for the headstage amplifier and would decrease both its open-circuit noise and the noise increment associated with holder–pipette capacitance at the input.

It should also be noted that the noise associated with the command potential will react with C_{hp} (but not with C_{iss}) to produce noise in the measured current that once again has a PSD that rises as f^2. The command potential is normally attenuated (typically by 10:1 to 50:1) to reduce the noise arising from digital-to-analog converters or function generators. At the present time this is generally sufficient to reduce this potential source of noise to negligible levels. As other noise sources are reduced, however, more attention to such noise may become necessary. It should also be pointed out that the resistors in the attenuator are themselves a part of the command potential noise; therefore, low valued resistors are preferred.

In addition to the mechanisms just described, noise associated with the patch pipette arises from several other sources. Three potentially important sources of noise are considered here: (1) noise arising from the lossy dielectric characteristics of the glass, (2) noise arising from the thermal voltage noise of electrode resistance (distributed) in conjunction with the distributed capacitance of the pipette wall, and (3) noise arising from the patch capacitance in series with the resistance (lumped) of the pipette. Finally, the noise of the membrane–glass seal is briefly discussed.

Dielectric Noise. Thermal fluctuations in lossy dielectrics generate noise, the magnitude of which can be related to the real part of the admittance of the dielectric material (i.e., the loss conductance) by the fluctuation–dissipation theorem. More specifically for a dielectric with relatively low losses, the PSD, $i_d^2(f)$, of the noise current can be expressed in terms of the dissipation factor, D (also called the loss factor), and the capacitance, C_D, of the dielectric,[9] that is,

$$i_n^2(f) = 4kTDC_D(2\pi f) \qquad \text{A}^2/\text{Hz} \tag{1}$$

Note that the PSD of the noise associated with the dielectric loss of the glass from which the pipette is fabricated is expected to rise linearly with frequency. In situations where the dielectric noise of the pipette dominates total noise, this expected spectral shape is usually quite well approximated (see [3] in this volume). The root mean square noise arising from the lossy dielectric for a given bandwidth, B, can then be computed as the square

[9] V. Radeka, *IEEE Trans. Nucl. Sci.* **NS-20,** 182 (1973).

root of the integral of Eq. (1) from dc to the cutoff frequency, that is,

$$\text{rms noise} = (4kTDC_D\pi B^2)^{1/2} \quad \text{A rms} \tag{2}$$

If it is assumed that the ratio of the inner and outer diameters of a pipette is approximately preserved during the pulling process, then for pipettes fabricated from glass with a given wall thickness the important parameters for determining dielectric noise are the dissipation factor, dielectric constant, and depth of immersion of the pipette tip into the bath. The importance of the dissipation factor is obvious from Eq. (1) and (2). The dielectric constant of the glass, its wall thickness, and the depth of immersion go together to determine C_D. A standard rule of thumb states that the capacitance associated with the pipette is about 1–2 pF per millimeter of immersion into the bath (in the absence of Sylgard coating), but this will, of course, depend on the dielectric constant of the glass and geometry and wall thickness near the tip.

We normally use glass with an outer diameter (OD) of 1.65 mm and an inner diameter (ID) of 1.15 mm (OD/ID $\cong$ 1.43). Assuming that these proportions are preserved as the glass is drawn out by pulling, pipettes fabricated from this glass should have a capacitance of about 0.15ε pF per millimeter of immersion, where ε is the dielectric constant of the glass (e.g., 3.8 for quartz, 4–5 for most borosilcates, 6–7 for aluminosilicates, about 7 for soda lime glass, and 7–10 for high lead glasses). For thin walled glass with an OD/ID ratio of 1.2 the capacitance should increase to about 0.30ε pF/mm of immersion, whereas for thick walled glass with an OD/ID of 2.0 the capacitance should drop to about 0.08ε pF/mm. Obviously these numbers are only approximate since the assumption that glass proportions remain constant during pulling is itself only approximately true; in particular we have observed that for some glasses (e.g., aluminosilicates) there is a pronounced thinning of the wall dimensions at the pipette tip. Moreover, as discussed below, coating the pipette with Dow Corning (Midland, MI) Sylgard 184 (which has a relatively low dissipation factor of about 0.006 and a dielectric constant of 2.9) will modify the capacitance (and dissipation factor) of the pipette.

From the above discussion and Eqs. (1) and (2) it is clear that if the OD/ID ratio and the depth of immersion are constant then the root mean square noise arising from the lossy dielectric will be proportional to $(D\varepsilon)^{1/2}$, that is, the lowest noise glass should minimize the product of the dissipation factor and the dielectric constant. For example, of the glasses we have been able to obtian and successfully pull, Corning 7760 has the lowest $D\varepsilon$ product ($D\varepsilon = 0.036$, $D = 0.008$, $\varepsilon = 4.5$). This is followed by 8161 ($D\varepsilon = 0.041$); 7040, 0120, EG-6, 1723, and 7052 are also reasonably low, with $D\varepsilon$

values of 0.048, 0.054, 0.056, 0.063, and 0.064, respectively. On the other hand, 7740 (Pyrex borosilicate) and 1720 (an aluminosilicate) are substantially higher with $D\varepsilon$ values of 0.133 and 0.194, respectively. Soda lime glasses have the highest $D\varepsilon$ product; 0.37 and 0.47 for R-6 and 0080, respectively.

Using Eq. (2) and assuming a "typical" OD/ID ratio of 1.43, it is instructive to compute the root mean square value of the dielectric noise for several types of glasses in a 10-kHz bandwidth (all values listed would be somewhat higher if the transfer function of an 8-pole Bessel filter were taken into account). For a 1 mm depth of immersion 7760 should produce about 0.16 pA rms in this bandwidth; 8161 would produce 0.18 pA rms; 7052 should produce about 0.21 pA rms. On the other hand, 7740 should produce about 0.31 pA rms, and the soda lime glasses R-6 and 0080 would produce 0.51 and 0.58 pA rms, respectively. Because with the assumption of a constant OD/ID ratio the value of C_D is a linear function of the depth of immersion, the root mean square noise in a given bandwidth should vary as the square root of immersion depth. Thus for a 2 mm depth of immersion all of these values would be increased by a factor of 1.4 (e.g., for 7760 the dielectric noise in a 10-kHz bandwidth would increase to about 0.23 pA rms). Clearly, with an excised patch it is advantageous to raise the pipette as close to the surface of the bath as possible, and with on-cell patches the bath should be as shallow as possible for the lowest noise. For example, if the depth of immersion was only 0.2 mm the noise contribution from dielectric loss in a 10-kHz bandwidth for a 7760 pipette would be 0.08 pA rms; for soda lime glass it would be about 0.25 pA rms.

Using thicker walled pipettes would reduce dielectric noise; for example, for an OD/ID ratio of 2.0 all of the above root mean square calculations would decrease to about 70% of the values listed. In addition, the above calculations do not include effects of Sylgard coating of the pipette. Even if pipettes were fabricated from materials with negligible dielectric loss, coating of the pipette with Sylgard (or some similar hydrophobic material) would be necessary for low noise recording since Sylgard can prevent the creep of a thin layer of solution up the outer wall of the pipette.[10] This can be the dominant source of noise in uncoated pipettes. Sylgard, however, confers additional advantages in terms of pipette noise. The Sylgard coating thickens the wall of the pipette and thus reduces its capacitance. Sylgard has a low dielectric constant of 2.9 and a dissipation factor of 0.0058, which is lower than that of most glasses used in the fabrication of patch pipettes. Thus, Sylgard coating can be expected to reduce the dielectric noise of the patch pipette. However, its effects will be

[10] Hamill *et al.*, *Pflugers Arch.* **391**, 85 (1981).

difficult to quantify theoretically since the thickness of the applied coating is quite nonuniform; in particular it is difficult to produce very thick coatings in the final few hundred microns near the tip. It is expected and has been confirmed experimentally that the improvement associated with Sylgard coating will be greatest for relatively high noise glasses, especially soda lime glass. Smaller improvements should be expected for low loss glasses, but Sylgard coating will somewhat improve the noise of all glasses.

We have measured the noise of many types of glass and find that the agreement of the measured noise and the theoretical noise predicted for their dielectric loss is quite good. Plots of root mean square noise in a 10-kHz bandwidth for pipettes fabricated from 19 types of glass as a function of DC_D (more precisely $D\varepsilon/W$, where W is the OD/ID ratio, normalized to our standard ratio) are given in [3] in this volume. The relationship is monotonic and generally consistent with the theoretical predictions presented above. The depth of immersion was 1.5–2 mm, and all pipettes were covered with a moderate coat of Sylgard. In most cases, the measured value is somewhat less than predicted from Eq. (2): for low loss glasses the measured noise is only very slightly less than predicted; however, for high loss glasses (most notably the soda lime glasses) the departure is substantially higher. It seems almost certain that these departures arise from the Sylgard coating, which should have its largest effect on high-loss glasses. Nevertheless, considering the effects of Sylgard, a slightly variable depth of immersion, and somewhat variable tip geometry, we consider the agreement between theory and measurement to be excellent.

If ways become available to fabricate pipettes from them, several other glasses offer potentially lower dielectric noise, for example, 7070 ($D\varepsilon = 0.01$) and particularly quartz. At the time of this writing it appears that the ability to pull quartz capillaries into patch pipettes may soon become available. The dissipation factor of Corning 7940 (fused silica) has been variously reported to be as low as 3.8×10^{-5} and as high as 4×10^{-4}; its dielectric constant is 3.8. Thus, the $D\varepsilon$ product is in the range of 0.00014 to 0.0015. Arbitrarily selecting a value of D equal to 0.0002 ($D\varepsilon = 0.00076$), as a reasonable estimate, indicates that for the same OD/ID ratio the root mean square dielectric noise should be 7 times less for quartz pipettes than for pipettes fabricated from 7760 for the same depth of immersion, for example, only 0.023 pA rms for a 10-kHz bandwidth and a 1 mm depth of immersion. For a depth of immersion of only 0.2 mm this value would fall to 0.011 pA rms.

Noise Arising from Distributed Pipette Resistance and Capacitance. The preceding discussion of dielectric noise might be taken to imply that pipettes fabricated from glass with very low dissipation factors might introduce only negligible amounts of noise into patch clamp measurements.

Unfortunately, however, the pipette has several other sources of noise that must be taken into account. One of these arises from the distributed resistance and capacitance of the pipette. In this section we consider the pipette capacitance to be lossless.

As described above, it is reasonable to assume that the capacitance of the pipette is more or less evenly distributed over the length of pipette immersed in the bath. On the other hand, the majority of the resistance of the pipette resides at or very near the tip. Nevertheless, a significant amount of resistance arises from the filling solution in the first few millimeters behind the tip. If the pipette is modeled as a shank region (with ID $\cong$ 1.2 mm) and a conical region approaching the tip with an angle of the cone of 11.4° (such that the ID increases to 100 μm at a distance 0.5 mm back from the tip, 200 μm at a distance of 1 mm from the tip, 400 μm at 2 mm, etc.) and a 1 μm diameter opening, then its total resistance should be about 3.2 MΩ when filled with a solution with a resistivity of 50 Ω cm. Of this about 2.4 MΩ will reside in the first 20 μm of the tip region; more than 3 MΩ will reside within the first 100 μm. However, significant resistances will be associated with regions further removed from the tip. For example, the region from 100 to 200 μm from the tip would have a resistance of 80 kΩ; the region from 200 to 300 μm from the tip would have a resistance of about 27 kΩ; and the region from 0.5 mm to 2 mm back from the tip would have a resistance of about 24 kΩ. Of course an Ag–AgCl wire extends into the solution in the pipette, and it is reasonable to assume that only a negligible amount of resistance is contributed by solution in the region into which the wire protrudes.

In any case, a feeling for the noise arising from this distributed capacitance and resistance can be gained by considering that roughly 0.5 pF of capacitance is associated with the final 0.5 mm of the electrode prior to the tip and perhaps 30 kΩ of resistance is associated with the pipette up to this point (i.e., the filling solution from the shank up to 0.5 mm from the tip). Clearly the 0.5 pF of capacitance is in series with this 30 kΩ. The 30-kΩ resistance has a thermal voltage noise PSD of about 22 nV/Hz$^{1/2}$ (about 10 times higher than the input voltage noise of a good headstage); in series with 0.5 pF this will produce current noise (PSD rises as f^2) which would have a magnitude of about 0.05 pA rms in a bandwidth of 10 kHz (8-pole Bessel filter) and 0.15 pA rms in a 20-kHz bandwidth.

Of course the actual situation is more complicated than this since both the pipette resistance and capacitance are distributed. Over the frequency range of interest to patch clamping the PSD (A^2/Hz) of this noise should rise approximately as f^2. If it is assumed that the resistance is negligible beyond 4 mm behind the tip (as would be expected if the Ag–AgCl—or particularly a platinized Ag–AgCl—wire protruded at least this close to

the tip), then with the pipette geometry assumed above and assuming a uniformly distributed capacitance of 1 pF per millimeter of immersion, rough calculations indicate that the total noise arising from this mechanism would be about 0.13 pA rms for a bandwidth of 10 kHz (−3 dB, 8-pole Bessel filter) and an immersion of 2 mm. For an immersion depth of only 1 mm this value would fall to about 0.1 pA rms. For an electrode modeled as above but with a cone angle of 22.6° (with a tip opening of 1 μm the total resistance would be 1.6 MΩ) and with other parameters as assumed above, the noise from this mechanism should roughly fall by half, namely, for a 10-kHz bandwidth to about 0.07 pA rms for a 2 mm immersion depth and about 0.05 pA rms for 1 mm of immersion.

The above calculations are highly approximate. Noise arising from this mechanism would be expected to increase if the wire—which has the effect of shunting a portion of the electrode resistance—did not protrude as far toward the tip. This would be particularly true if there were any extended region behind the tip where the electrode taper became very shallow and resulted in significantly increased resistance distal to the tip. More generally, it seems clear that the geometry of the first few millimeters behind the tip will have important effects on this noise. It should also be noted that withdrawing the tip toward the surface would not reduce this noise as much as might be expected; this would decrease the capacitance of the pipette but not the resistance.

There should also be ways of reducing the noise arising from this mechanism. For even the best glasses presently used in patch clamping this might not seem particularly important since dielectric noise should be larger than the rough predictions listed above. However, as techniques become available to fabricate pipettes from lower loss glass, such reductions would be expected to take on greater significance. First, Sylgard coating can significantly reduce pipette capacitance. However, there are some limitations to this reduction in the first few hundred microns behind the tip since it is difficult to build up a thick coat of Sylgard in this region. Thicker walled glass would also reduce pipette capacitance. The use of glass with a low dielectric constant can also reduce the noise from this mechanism; for an OD/ID ratio of approximately 1.43, quartz ($\varepsilon = 3.8$) should have a capacitance of about 0.6 pF/mm of immersion and 7760 should have about 0.7 pF/mm. It should be noted that root mean square noise from this mechanism in a given bandwidth is expected to decrease linearly with decreasing capacitance per unit length. Finally, it should be possible to reduce this noise significantly without respect to the depth of immersion by using a fine wire (platinized Ag–AgCl would be preferred in this case) protruding as close to the tip as possible. For example, a 100 μm diameter wire slightly sharpened at the tip should be able to be advanced to within

0.5–1 mm of the tip. This would in effect short out the resistance of the pipette in the region into which the wire protrudes; the reduction of impedance would be frequency dependent but should be quite effective by 1 kHz. This should reduce noise from distributed pipette resistance and capacitance even if the pipette were immersed further than the wire extended toward the tip: the wall capacitance would remain (with its dielectric noise) in regions where the wire and bath overlap, but the resistance—and its thermal voltage noise—would be greatly reduced.

In summary, it should be possible to reduce noise associated with the distributed pipette resistance and capacitance to roughly 0.03 pA rms in a 10-kHz bandwidth by careful control of pipette geometry, use of low dielectric constant glass, careful coating with Sylgard, and using a fine wire protruding as close to the tip as possible. A minimum depth of immersion is also desirable. Although these precautions are probably unnecessary at the present time, they could become important as other sources of noise are reduced. In particular, for very low loss glasses (e.g., quartz) this mechanism would exceed dielectric noise.

Noise Arising from Lumped Pipette Resistance and Patch Capacitance. The entire resistance of the pipette is in series with the capacitance of the patch membrane. This series combination will lead to a current noise with a PSD denoted by $i_{pc}^2(f)$ that should be given by

$$i_{pc}^2(f) = 4\pi^2 e_p^2 C_p^2 f^2 \tag{3}$$

where e_p^2 is the PSD of the voltage noise of the pipette resistance, R_p ($e_p^2 \cong 4kTR_p$), and C_p is the patch capacitance. Typical values of R_p range from about 1 to 10 MΩ. The value of C_p has been measured by Sakmann and Neher[11] to fall in the range of 0.01 to 0.25 pF. They found that despite a large amount of scatter, C_p was correlated with R_p. As expected C_p increased as R_p decreased; they estimated C_p to typically be 0.126 pF($1/R + 0.018$), where R is the electrode resistance in megohms. This would imply that "typically" for R_p values of 10, 5, 2, and 1 MΩ, C_p would be 0.015, 0.027, 0.065, and 0.128 pF, respectively; the root mean square noise in a 10-kHz bandwidth (8-pole Bessel filter) would be 0.03, 0.04, 0.06, and 0.08 pA rms, respectively, that is, typical noise form this mechanism would increase as R_p decreased. From the results of Sakmann and Neher it can also be predicted that even less noise is sometimes generated from R_p and C_p; in the most favorable situations in terms of noise ($R_p = 2.5–3$ MΩ, $C_p \cong 0.01$ pF) this noise is only about 0.01 pA rms in a 10-kHz bandwidth.

[11] B. Sakmann and E. Neher, eds., "Single-Channel Recording," p. 37. Plenum, New York and London, 1983.

However, in the least favorable situations (when a large bleb of membrane has been drawn into the pipette, e.g., $R_p \cong 2$ MΩ, $C_p \cong 0.25$ pF) the noise from this mechanism can be as high as 0.22 pA rms in a 10-kHz bandwidth. Clearly, the lowest amount of R_p–C_p noise will result from situations in which relatively little membrane in drawn into the pipette. Pipette geometries favoring this situation may not be optimal in terms of the distributed pipette resistance and capacitance noise considered in the previous section.

Seal Noise

The final mechanism of noise associated with the pipette which we will consider here is the noise associated with the membrane–glass seal. The seal resistance will be denoted by R_{sh}. If the only noise associated with the seal was the thermal current noise of R_{sh}, then for zero applied field across the seal the noise PSD arising from the seal would be given by $4kT/R_{sh}$. In a 10-kHz bandwidth this would amount to 0.4, 0.13, 0.04, and 0.028 pA rms for seal resistances of 1, 10, 100, and 200 GΩ, respectively. It should be noted that we have with some cell types frequently achieved seal resistances of 50–200 GΩ or more, whereas with other cell types typical seal resistance can be as low as 2–10 GΩ. Exceptional noise performance can only be obtained with very high resistance seals.

The simple assumption that seal noise can be approximated by the thermal current noise of R_{sh} may well be incorrect. More generally, the noise at equilibrium will be defined by $4kTRe\{Y_{sh}\}$, where $Re\{Y_{sh}\}$ is the real part of the seal admittance. Because the precise nature of the membrane–glass seal is unknown, we do not know how to estimate Y_{sh}. Clearly, the assumption that $Re\{Y_{sh}\} = 1/R_{sh}$ is a minimum estimate of noise. It is certainly possible that the PSD of the noise of the seal rises with increasing frequency owing to the capacitance of the glass and particularly of the membrane which makes up the wall of the seal.

Seal resistances of 100–200 GΩ are not uncommon. Using macroscopic calculations with reasonable estimates of the area involved in the seal thus leads to estimates of the separation between the membrane and the glass of the order of 0.1 Å. Such a result only indicates that macroscopic calculations of this sort are inappropriate. We therefore have no clear idea of how to model the seal electrically or precisely predict its noise. Moreover, it seems virtually impossible to dissect out the seal noise from patch clamp measurements empirically. Previous attempts to do this certainly overestimate this noise. For example, data from Sachs and Neher reported in Sigworth[5] indicate that the seal would produce a noise of about 0.13 pA rms in a 5-kHz bandwidth (assuming a very sharp filter cutoff;

with a Bessel filter this estimate should increase to at least 0.16 pA rms), whereas we have on many occasions achieved less noise than this for the entire system (headstage, holder, pipette, seal, etc.) in the same bandwidth. Besides, their measurement of seal noise would have included the R_s–C_p noise described above. We can only put an upper bound on seal noise by a root mean square subtraction of all noise sources we can account for from the total measured noise. For our lowest noise patches to date this upper bound is about 0.05–0.06 pA rms in a 5-kHz bandwidth.

Summary of Noise Sources and Limits of Noise Performance

Headstage. At the time of this writing, the best capacitive feedback headstages have noise of about 0.18 pA rms in a 10-kHz bandwidth (8-pole Bessel filter). As already noted, however, it seems possible that with present technology this could be reduced to as little as 0.06–0.10 pA rms. At present the input voltage noise, e_n, of the best available headstages is about 2 $nV/Hz^{1/2}$. Reduction of this value is also possible and will be important in reducing the noise contributed by the holder and pipette.

Holder. By itself, a well-designed holder adds relatively little noise to patch clamp measurements provided that it is periodically cleaned and maintained free of pipette filling solution. A holder which is not covered with metallic shielding will typically add only 1–2 pF of capacitance to the headstage input. If the holder is fabricated from a low-loss dielectric material this capacitance in conjunction with the input voltage noise of the headstage will be the dominant source of noise associated with the holder. It can be expected to increase the noise by about 10% over that of the headstage alone. For a good capacitive feedback headstage with 0.18 pA rms noise in a 10-kHz bandwidth, the noise should not increase to more than about 0.20 pA rms by the addition of the holder. For a headstage with lower e_n than is presently available both the open-circuit headstage noise and the noise increment associated with the holder will decrease.

Of course the holder will also produce some dielectric noise. However, for low-loss dielectric materials this is not expected to be too severe. In the future, as other sources of noise decline, the construction of the holder (and input connector) may need to be reevaluated to reduce dielectric noise further.

Pipette. The first mechanism to consider in terms of pipette noise is simply the lumped capacitance of the pipette in series with the input voltage noise of the headstage. As was the case with the holder, this noise is perfectly correlated with noise arising from e_n and the headstage input capacitance, and therefore the usual rules of root mean square addition of uncorrelated noise sources do not apply. The pipette can add 1–5 pF of

capacitance to the headstage input, with the lowest values being associated with low dielectric constant glass, thick walled pipettes, heavy Sylgard coating, and a shallow immersion of the tip into the bath. With proper precautions this source of noise need not increase total noise by more than about 5–10% above that of the headstage–holder combination.

Three other sources of noise associated with the pipette were also described above and are briefly summarized here.

Dielectric Noise. At present, dielectric noise is probably the dominant source of noise for all but the very best glasses available. All else being equal, this noise will be the smallest for glasses with the smallest product of their dissipation factor, D, and dielectric constant, ε. This noise will also be minimized by using relatively thick walled pipettes, shallow depths of immersion, and, particularly for relatively lossy glasses, a heavy coating of Sylgard. Of commonly used glasses, Corning 7760 has the smallest value of $D\varepsilon$ of 0.036. With 7760 it can be expected that a noise component of about 0.2 pA rms in a 10-kHz bandwidth will result from a 1.5–2 mm immersion with "standard" wall thickness glass and a moderate coat of Sylgard. For thicker walled glass and shallower depths of immersion this value could fall to 0.06–0.08 pA rms.

It may soon become possible to fabricate patch pipettes from very low-loss (high melting temperature) glasses, most notably quartz. For quartz, the $D\varepsilon$ product is approximately 0.0008, and dielectric noise would be expected to fall to about 0.03 pA rms for a 1 mm depth of immersion.

Distributed Pipette Resistance and Capacitance. The capacitance of the pipette is more or less evenly distributed over the length which is immersed in the bath. The pipette resistance is located primarily at or very near the tip, but significant resistance still resides in the first few millimeters behind the tip. The thermal voltage noise of this distributed resistance in conjunction with the distributed capacitance of the pipette is a potentially large source of noise. Rough calculations indicate that for a 1–2 mm depth of immersion this noise source should produce 0.05–0.13 pA rms noise in a 10-kHz bandwidth for pipettes with relatively ideal geometry. For less ideal pipettes (particularly ones with relatively higher resistance more distal to the tip) the noise contribution could easily be larger. This noise should be minimized by using thick walled glass with a low dielectric constant, relatively heavy Sylgard coating, and careful control of pipette geometry. Extending a slender Ag–AgCl or platinized Ag–AgCl wire as close as possible to the tip, thereby shorting out most of the resistance up to the end of the wire, could also reduce this source of noise.

R_p–C_p Noise. The capacitance of the patch membrane is in series with the entire pipette resistance. The thermal voltage noise of the pipette resistance produces current noise with the patch capacitance. This noise

will generally be quite small, but it can become significant when the area of the patch is large. Values can be as little as 0.01 pA rms in a 10-kHz bandwidth but can exceed 0.2 pA rms in the same bandwidth for large patches. A value of 0.05 pA rms in a 10-kHz bandwidth could be considered to be "typical" for a pipette of 3–5 MΩ.

Seal Noise

The noise associated with the seal is probably the most poorly understood of all noise sources in the patch voltage clamp technique. We have argued that previous attempts to quantify this noise almost certainly overestimate its value, but it is well known to anyone who has spent much time trying to achieve low noise measurements that there is a large degree of variability in total noise from seemingly identical recording situations, even when the dc seal resistance is very high. Because this variability is too large to be readily accounted for on the basis of the quantifiable sources of noise described above, it seems reasonable to blame it on the seal.

The minimum noise PSD associated with the seal in the presence of zero applied voltage is given by $4kT/R_{sh}$, where R_{sh} is the dc seal resistance; the root mean square value in a bandwidth, B, is given by $(4kTB/R_{sh})^{1/2}$. For a 100-GΩ seal this would amount to 0.04 pA rms in a 10-kHz bandwidth. It seems likely that the actual seal noise is larger than this, but we have no good theoretical basis on which to estimate total seal noise. From our lowest noise patches (with $R_{sh} \geq 50$ GΩ) we can estimate that an upper bound for seal noise is about 0.05–0.06 pA rms in a 5-kHz bandwidth and 0.10–0.12 pA rms in a 10-kHz bandwidth. Of course similar estimates for higher noise patches would yield higher values.

Limits of Noise Performance

With a headstage with a noise of 0.18 pA rms in a 10-kHz bandwidth we can predict that the best total noise that can be achieved at present is about 0.25 pA rms (10 kHz, 8-pole Bessel filter). This estimate arises from assuming that the noise associated with the holder and the lumped capacitance of the pipette increases the noise to 0.20 pA rms and assumes the following values for other (uncorrelated) noise sources (all in a 10-kHz bandwidth): dielectric noise; 0.08 pA rms; distributed resistance-capacitance pipette noise; 0.07 pA rms; R_s–C_p noise; 0.02 pA rms; seal noise, 0.10 pA rms. The total is thus $(0.20^2 + 0.08^2 + 0.07^2 + 0.02^2 + 0.10^2)^{1/2}$, or approximately 0.25 pA rms. This is in good agreement with our best results to date.

It is worth noting that the headstage itself is the dominant source of noise in this situation; if headstage noise were reduced to zero, the total

noise would be expected to fall to about 0.15 pA rms. With improved techniques it should be possible to reduce the dielectric noise of the pipette to 0.03 pA rms and the noise from the distributed resistance and capacitance of the pipette to a similar value, both in a 10-kHz bandwidth. It is also possible that seal noise might be as low as 0.03–0.05 pA rms in this bandwidth; using 0.04 pA rms as an optimistic (probably overly optimistic) estimate, it seems possible that under ideal circumstances all noise not directly associated with the headstage might produce as little as 0.06 pA rms in a 10-kHz bandwidth. With a headstage that contributes 0.20 pA rms, such improvements might hardly seem worthwhile since best case total noise would only fall from 0.25 to 0.21 pA rms. However, with a headstage with a total noise contribution of only 0.08 pA rms, total noise could fall to as little as 0.10 pA rms in a 10-kHz bandwidth. Thus, at least to our minds, further efforts to reduce both the noise of the electronics and noise associated with the pipette seem worthwhile and could be expected to reduce noise levels by a factor of 2 or somewhat more below the best that can be achieved at the present time.

Whole Cell Voltage Clamping

In the whole-cell variant of the patch voltage clamp technique direct access to the cell interior is provided by disrupting the patch membrane after the formation of a gigohm seal. Disruption is accomplished by either applying additional suction to the pipette or by applying a brief high voltage pulse (e.g., 1 V) to the pipette. If the procedure is successful the gigohm seal remains and the interior of the patch pipette directly communicates with the interior of the cell. An alternative approach is the so-called perforated patch technique in which the pipette contains amphotericin or nystatin; these channels incorporate into the patch membrane and, over a period of some 10 to 20 min, provide a low access resistance from the pipette to the cell interior. With either approach it is not uncommon to find that the final access resistance is 2 or even 3 times as large as the original resistance of the pipette. After a sufficient period of time the access resistance of the perforated patch technique can become quite stable. However, it is often found that following disruption of the patch the access resistance is not stable; if this is the case the resistance will typically increase with time.

Most of the general characteristics of the dynamic and noise performance of the whole-cell configuration of the patch voltage clamp are now well known and will not be elaborated here. Instead, we focus our attention on the effects of the access or series resistance arising from the pipette. The access resistance associated with the pipette is in series with the membrane

capacitance of the cell being voltage clamped. This has very important effects on voltage errors associated with the flow of transmembrane current, on the actual bandwidth of the current measurement, and on the noise associated with the whole-cell voltage clamp.

Dynamic Effects of Series Resistance

It is well known that the pipette resistance, R_s, causes a voltage error in the presence of transmembrane ionic current, i_m, with a magnitude given by $i_m R_s$. With an access resistance of 10 MΩ, an ionic current of 2 nA will result in a 20-mV error in the absence of series resistance compensation. Such errors are compounded when dealing with voltage-activated channels. For example, inward currents through voltage-dependent sodium channels will lead to depolarizing error voltages which in turn will activate more channels. Thus, the whole-cell voltage clamp technique is often inadequate to study cells with large, voltage-dependent ionic currents. A typical mammalian ventricular myocyte, for example, can have sodium currents of 10 nA or more, and with an R_s of 10 MΩ it is necessary to compensate for 90–95% of this resistance to achieve marginally adequate voltage control.

It is also well known that uncompensated series resistance in conjunction with membrane capacitance will cause the true transmembrane potential, V_m, to respond to a step change of command potential, V_c, with a time course given by $V_m = V_c[1 - \exp(-t/\tau_s)]$, where $\tau_s = R_s C_m$. For $R_s = 10$ MΩ and $C_m = 50$ pF, $\tau_s = 500$ μsec, and it will require a V_m of about 2.3 msec to settle to within 1% of its final value following a step change in V_c. The capacity transient (prior to use of "whole-cell compensation" provided on most commercial patch clamps) has the shape of the derivative of the membrane potential, V_m.

Aside from this delay in establishing the desired transmembrane potential, it is often assumed that when studying relatively small ionic currents (say a few hundred pA) in the whole-cell configuration of the patch clamp series resistance presents no major limitations. Unfortunately, this ignores another important effect of series resistance, namely, the filtering effect of series resistance and membrane capacitance on the measured current. In the absence of series resistance compensation, the measured current is effectively filtered by a one-pole (RC) filter with a corner (−3 dB) frequency given by $1/(2\pi R_s C_m)$. Whether this filtering is important, of course, depends on the highest frequency components of interest in the signal to be measured.

In extreme situations this bandwidth restriction can be quite severe. For example, for a large cell with $C_m = 200$ pF, an uncompensated series

resistance of 10 MΩ will reduce the effective bandwidth of current measurement to only about 80 Hz. For a more or less typical situation with $R_s = 10$ MΩ and $C_m = 50$ pF, the effective bandwidth is about 320 Hz, which is still too small for many types of measurements. In a more ideal situation with a small cell with $C_m = 10$ pF and a relatively low access resistance of 5 MΩ, the effective bandwidth is increased to about 3.2 kHz. In any case, setting the bandwidth of the external filter used with the patch clamp to much more than the bandwidth limitation imposed by R_s and C_m will not provide significant additional information about the current signal. It will, however, provide extra noise (see below).

Although open-loop techniques such as "supercharging" [12] can speed up the response time of the membrane potential, the only way to increase the bandwidth limitation is to employ series resistance compensation. Such compensation will reduce the effective resistance in series with the membrane from R_s to R_{sr}, where R_{sr} is the residual (uncompensated) series resistance. For example, with $R_s = 10$ MΩ, 80% compensation means that R_{sr} is 2 MΩ. In this situation the bandwidth limitation is increased to $1/(2\pi R_{sr} C_m)$. Thus, using "typical" parameters of $R_s = 10$ MΩ and $C_m = 50$ pF, 70% series resistance compensation will increase the effective bandwidth to about 1060 Hz; 80% compensation increases this bandwidth to about 1600 Hz; 90% compensation increases this further to about 3.2 kHz.

It must be noted, however, that achievement of series resistance compensation of 90% or better in whole-cell voltage clamping is often difficult and sometimes impossible. Even if such levels can be achieved, the response is often no longer first order so that the simple bandwidth calculations presented above will no longer be strictly accurate. Moreover, most commercial patch clamps provide a "lag" control to be used with series resistance compensation. Use of lag puts the signal fed back to compensate for series resistance through a filter (usually first order). In effect, this means that series resistance is only compensated up to some bandwidth determined by the lag circuit. For a "10-μsec lag" this bandwidth is 16 kHz. However, for a 100-μsec lag the bandwidth of series resistance compensation is reduced to only 1.6 kHz. The overall bandwidth of current measurement achieved by series resistance compensation is, of course, affected by the use of lag. Clearly, if wide bandwidths are desired the lag control should be set to the minimum level necessary to achieve stability.

It should also be noted that when series resistance compensation is used it is important to use "fast capacity compensation" to eliminate currents involved in charging stray and pipette capacitance at the headstage input.

[12] R. H. Chou and C. M. Armstrong, *Biophys. J.* **52**, 133 (1987).

Because this capacitance is not associated with any significant series resistance its effects must be eliminated if series resistance compensation is to be stable.

Noise Associated with Series Resistance in Whole-Cell Voltage Clamps

At moderate to high frequencies the noise performance of the whole-cell variant of the patch voltage clamp technique is generally dominated by current noise arising from the voltage noise of the series (pipette) resistance, R_s, in conjunction with the cell membrane capacitance, C_m. The power spectral density (PSD) of the voltage noise of the pipette excluding $1/f$ noise is given by

$$e_s^2 = 4kTR_s \qquad V^2/Hz$$

where k is Boltzmann's constant and T is the absolute temperature. For $R_s = 10$ MΩ, e_s is about 400 nV/Hz$^{1/2}$ which is more than 100 times the input voltage noise of a high quality headstage (2–3 nV/Hz$^{1/2}$ at frequencies above 1 kHz or so). In addition, $1/f$ noise will be associated with the pipette, particularly when current is flowing through it.[13] Even for an R_s of 1 MΩ the noise of the electrode will be at least 126 nV/Hz$^{1/2}$. Because this noise is directly in series with the headstage input voltage noise it should be obvious that the voltage noise of the electronics is irrelevant to noise performance in whole-cell voltage clamping. As will be seen below, the noise of the feedback resistor (typically only about 500 MΩ for whole-cell clamping) is also generally irrelevant to overall noise for all bandwidths above a few hundred hertz.

The power spectral density of the current noise arising from the electrode voltage noise (again ignoring any $1/f$ component) and the whole-cell membrane capacitance is given by

$$\text{PSD} = (4\pi^2 f^2 e_s^2 C_m^2)/(1 + 4\pi^2 f^2 \tau_{sr}^2) \qquad A^2/Hz \qquad (4)$$

where f is the frequency in hertz, $\tau_{sr} = R_{sr}C_m$, and R_{sr} is the residual (uncompensated) series resistance. If it were possible to compensate for 100% of series resistance then R_{sr} would be zero and Eq. (4) would simplify to $4\pi^2 f^2 e_s^2 C_m^2$. Because it is generally not possible to achieve series resistance compensation levels much above 90% without introducing excessive ringing into the capacitive current, the full form of Eq. (4) should generally be used. Note that the form of the power spectral density rises (as f^2) with increasing frequency and then plateaus at frequencies above $1/(2\pi\tau_{sr})$. The

[13] L. J. DeFelice and D. P. Firth, *IEEE Trans. Biomed. Eng.* **18**, 339 (1971).

high frequency asymptote is given by $e_s^2 C_m^2/\tau_{sr}^2$. As an example, consider a cell with $C_m = 50$ pF voltage clamped through a series resistance of 10 MΩ (recall that this is typical for pipettes with an original resistance in the range of 3–5 MΩ). Without any series resistance compensation the actual bandwidth of current measurement is limited to about 320 Hz [$1/(2\pi R_s C_m)$]. By a frequency of 100 Hz the current noise power spectral density has risen to 1.6×10^{-28} A²/Hz which is equivalent to the thermal current noise of a 100-MΩ resistor; indeed at any frequency above about 45 Hz the noise PSD from this mechanism will exceed that of a 500-MΩ resistor, which is the typical value used in commercial patch clamps for whole-cell measurements. At frequencies above 320 Hz the noise PSD approaches a steady level of 1.6×10^{-27} A²/Hz which is equivalent to the noise of a 10-MΩ resistor. An external filter must be used to roll off this noise; a cutoff frequency much larger than 320 Hz is not justified on the basis of the effective *signal* bandwidth limitation introduced by the series resistance.

When series resistance compensation is employed the value of τ_{sr} is decreased and the noise power spectral density continues to rise to higher frequencies. For example, with the same parameters just considered 90% series resistance compensation will produce an effective signal bandwidth of 3200 Hz, and the noise will continue to rise up to this frequency; by 1000 Hz the noise PSD reaches 1.6×10^{-26} A²/Hz (equivalent to the current noise of a 1-MΩ resistor), and the high frequency plateau will reach 1.6×10^{-25} A²/Hz (equivalent to the current noise PSD of a 100-kΩ resistor). With about 97% compensation (if this could be achieved) the effective signal bandwidth would increase to 10 kHz, and the high frequency asymptote of the noise would reach a level equivalent to the PSD of a 10-kΩ resistor (1.6×10^{-24} A²/Hz). Assuming that sufficient series resistance compensation is used to extend the effective signal bandwidth to somewhat more than the −3 dB bandwidth of an external 8-pole Bessel filter the noise expected from this mechanism alone will be somewhat more than 3 pA rms (about 18 pA peak to peak) for a filter cutoff frequency of 1 kHz. This would increase to 9 and about 36 pA rms (about 220 pA peak to peak) for filter bandwidths of 2 and 5 kHz, respectively. These values are equivalent to the root mean square current noise arising from resistances of about 1.5 MΩ, 400 kΩ, and 60 kΩ for the bandwidths 1, 2, and 5 kHz, respectively. It is obvious in this situation that the electronics will contribute only a very tiny fraction of the overall noise at any of these filter settings even if the feedback resistor were only 50 MΩ.

For any particular cell, that is, for any particular value of membrane capacitance, the only way to reduce the noise arising from the access resistance is to reduce the access resistance itself. In the specific example

considered above the value of R_s was 10 MΩ. For a value of R_s of 2.5 MΩ with the same value of C_m (50 pF) the root mean square noise values listed above would be reduced by a factor of 2. Pipettes can be fabricated from several types of glass with tip geometries intended to minimize R_s (see [3], this volume). Unfortunately, however, in our experience, even with seemingly ideal pipettes it is relatively rare to establish stable whole-cell recordings with access resistances much below 2–3 MΩ. Thus when series resistance compensation is used to extend the signal bandwidth above $1/2\pi R_s C_m$ large levels of noise must be anticipated. It is important to note that series resistance compensation restores the high frequency components of both the signal and the associated noise. In a well-designed system the increase in noise is only the restoration of the noise that would have been present as a result of the series combination of the electrode voltage noise and cell capacitance in the absence of the filtering effects of R_s already described.

The specific example used above (i.e., $R_s = 10$ MΩ, $C_m = 50$ pF) may seem overly pessimistic. However, worse situations, in terms of both noise and the need for series resistance compensation, have been reported in the literature. For example, mammalian ventricular myocytes often have capacitances as large as 200–300 pF and have been clamped with access resistances of 10 MΩ or more. Nevertheless, it is worth briefly considering a more ideal situation, namely, a small cell with $C_m = 5$ pF and a relatively low value of R_s of 5 MΩ (e.g., chromaffin cells, see Marty and Neher[14]). The bandwidth limitation arising from C_m and completely uncompensated R_s is 6.4 kHz in this case, which is large enough for most whole-cell measurements. The power spectral density of the noise arising from R_s and C_m is, of course, much less than in the previous example. However, it will still exceed the PSD of the thermal current noise of a 500-MΩ resistor (typical for whole-cell voltage clamps) at all frequencies above about 640 Hz. At a frequency of 1 kHz the "R_s–C_m" noise is equivalent to the current noise PSD of a 200-MΩ resistor, and by about 5 kHz it has risen to a level equivalent to an 8-MΩ resistor. Thus, even in this situation it is obvious that except at rather narrow bandwidths (less than about 1 kHz) the noise of the feedback resistor will not dominate total noise. For a bandwidth of current measurement of 5 kHz, the root mean square noise arising from R_s and C_m (5 MΩ and 5 pF) will be at least 6 times greater than that of a 500-MΩ resistor in the same bandwidth, so that the total

[14] A. Marty and E. Neher, *in* "Single-Channel Recording" (B. Sakmann and E. Neher, eds.), p. 107. Plenum, New York and London, 1983.

noise would be reduced by only about 1% by completely eliminating the noise of the feedback resistor.

Filter

Filter characteristics are important in determining the amount of noise present in a given measurement and the resolution of the signal. Obviously, the bandwidth of a filter is adjusted to reduce noise to tolerable levels so that the desired signal can be adequately observed. Filtering prior to digitization is also required to prevent aliasing (see discussion in next section). When the desired signal is large relative to the background noise, the selection of filter bandwidth (and digitization rate) can be determined simply on the basis of the time resolution required in the measurement; wider bandwidths, of course, allow the observation of more rapid events. However, when the signal-to-noise ratio is relatively small, compromises between the amount of noise that is allowed and the time resolution achieved are often necessary. This second situation is usually the case for single-channel recordings.

The ideal filter would be one which possesses both a sharp cutoff in the frequency domain as well as a rapid smooth settling step response in the time domain. Unfortunately such a filter is theoretically impossible. There are well-defined limits on the degree to which a signal can be simultaneously "concentrated" in both the time domain and the frequency domain. Filters with narrow smooth impulse responses and therefore rapid rise times with minimal overshoot have rather gradual roll-offs in the frequency domain, whereas filters with a sharp cutoff in the frequency domain will be characterized (for the same -3 dB bandwidth) by more spread out impulse responses and a step response with a slower rise time and rather severe overshoot and ringing.

Of commonly used filter types, the Gaussian and Bessel filters provide the best resolution with minimum overshoot and ringing of the step response. The impulse response of a Gaussian filter has the shape of the Gaussian distribution. It has an essentially ideal step response with no overshoot; its 10–90% rise time is approximately $0.34/f_c$, where f_c (Hz) is the -3 dB bandwidth, and it settles to within 1% of its final value in about $0.8/f_c$ sec. Unfortunately, in the frequency domain the roll-off of a Gaussian filter is rather gradual. If the transfer function of a filter is denoted by $H(f)$, then for a Gaussian filter at $f = f_c$, $H(f) = 0.707$ (-3 dB); at $f = 2f_c$, $H(f) = 0.25$ (-12 dB); at $f = 3f_c$, $H(f) = 0.044$ (-27 dB); and at $f = 4f_c$, $H(f) = 0.004$ (-48 dB). An eighth order Bessel filter closely approximates the response of a Gaussian filter in both the time and the frequency

domains; in fact as the order of the Bessel filter becomes large the two filters become essentially identical.

From the point of view of noise reduction at high frequencies, it would be desirable to have a filter with a transfer function that rolls off much more rapidly after it reaches f_c. A wide variety of analog filters with such characteristics are available (e.g., Chebyshev and elliptical filters). In fact, analog filters which have rolled off to $H(f)) = 0.01$ (−40 dB) by $f = 1.06f_c$ are available, and digital filters can achieve even sharper cutoffs. Unfortunately such sharp cutoff filters have very undesirable characteristics in the time domain. In particular, for the same f_c their rise time will be longer than that of a Gaussian or Bessel filter, and their step response will have a large overshoot and prolonged ringing. For example, the step response of an eighth order Chebyshev filter (0.5 dB ripple) will have a 10–90% rise time of about $0.55/f_c$ (i.e., about 1.6 times that of a Gaussian or Bessel filter), a peak overshoot of about 23%, and would require more than $8/f_c$ sec to settle to within 1% of its final value. An eighth order Butterworth filter has frequency domain performance that can be thought of as lying between that of the Gaussian and Bessel types and the extremely sharp cutoff filters such as Elliptical and Chebyshev. Nevertheless, its time domain performance is rather poor, and these filters should also generally be avoided for most patch clamp studies.

To achieve their excellent performance in the frequency domain, sharp cutoff filters have sacrificed time domain performance. In fact, if we operationally define the time domain resolution of a filter as $1/T_r$, where T_r is the 10–90% rise time, it would be found that in order to achieve the same time resolution with a sharp cutoff filter as that achieved with a Gaussian or Bessel filter it is necessary to use a higher value of f_c for the sharp cutoff filter. In this case the sharp cutoff filter would generally pass as much or more noise than the Gaussian or Bessel filter if they have been set to achieve essentially the same time resolution. Thus, the presumed noise advantage of sharp cutoff filters is an illusion if the objective is to achieve the minimum noise for a given time resolution. Although some rather exotic filter types can provide the same rise time with minimal overshoot as the Gaussian or Bessel filter and reduce typical patch clamp noise by a small amount, the improvement is only a few percent with realistic noise power spectral densities.

Thus the Gaussian filter or a high order Bessel filter is the best choice for most patch clamp work. Although it is quite simple to produce a digital Gaussian filter, this type is more difficult to produce with analog electronics. Thus Bessel filters (fourth or preferably eighth order) are typically used with patch voltage clamps. There are many commercial sources of highly adjustable Bessel filters which are quite inexpensive. Several commercial

patch clamps also provide Bessel filters with a few values of f_c as an integral part of the instrument.

Aliasing

The sampling theorem states that a signal can be completely determined by a set of regularly spaced samples at intervals of $T = 1/f_s$ (where f_s is the sampling frequency) only if it contains no components with a frequency greater than or equal to $f_s/2$. Here we will denote $f_s/2$ by f_n; f_n is often called the Nyquist or folding frequency. Another way of stating the sampling theorem is that, for data sampled at evenly spaced intervals, frequency is only defined over the range from 0 to f_n. Noting that at least two points per cycle are required to define a sine wave uniquely, it should be obvious that components with frequencies higher than f_n cannot be described. Of course, there is nothing to stop an experimenter from digitizing a signal (plus noise) with frequency components that extend far beyond f_n. If this is done, it is reasonable to wonder what will happen to those frequency components above f_n in the final digitized data. The answer is that higher frequency components "fold back" to produce "aliases" in the range of frequencies from 0 to f_n.

The Nyquist frequency, f_n, is also referred to as the folding frequency because the frequency axis of the signal plus noise power spectral density will fold around f_n in a manner similar to folding a carpenter's scale. Frequency components lying above f_n are shifted to frequencies below f_n. If the frequency of a signal or noise component above f_n is denoted by f_x, then the frequency of its alias, f_a ($0 \le f_a \le f_n$) is given by

$$f_a = |f_x - kf_s|$$

Where f_s is the sampling frequency, k is a positive integer which takes on whatever value required so that f_a will fall into the frequency range from 0 to f_n (recall $f_n = f_s/2$), and the vertical bars indicate absolute value. For example, with $f_s = 10$ kHz ($f_n = 5$ kHz), a frequency component at 19 kHz will alias to a component at 1 kHz ($f_a = |19 \text{ kHz} - 2 \times 10 \text{ kHz}| = 1$ kHz). Similarly, frequency components at 9, 11, 19, 21, 29, 31, 39 kHz, etc., will all produce aliases at 1 kHz in the sampled data. Antialiasing filters are used when digitizing data to eliminate such aliases by attenuating the amplitude of all frequency components of the signal (plus noise) to negligible levels at frequencies above f_n.

We now present two examples of aliasing to show the kinds of problems it can create. First, consider noise with a white (i.e., constant) power spectral density of 10^{-14} V^2/Hz (100 $nV/Hz^{1/2}$) extending from dc to a sharp cutoff at 1 MHz. The total noise in a 1-MHz bandwidth is 100 μV

rms or about 0.6 mV peak to peak. If this noise were sampled at a rate of 1 point per 100 μsec ($f_s = 10$ kHz) without the use of an antialiasing filter, a little reflection should indicate that the root mean square (or peak-to-peak) value of the sampled points will be the same as it was in the original data, namely, 100 μV rms. However, the sampled data cannot describe frequency components that are greater than 5 kHz, that is, greater than f_n. In fact, if a smooth curve were fitted through the sampled points it would be found that the noise process appeared to be band limited from dc to 5 kHz but that its amplitude was the same as in the original data. The PSD of the sampled data will have increased to 2×10^{-12} V^2/Hz (1.4 μV/Hz$^{1/2}$), which is 200 times greater than that of the original data, because the act of sampling at 10 kHz had folded over the original PSD 200 times; all frequency components above f_n (5 kHz) have been aliased into the range from dc to 5 kHz.

It is important to note that the effects of aliasing cannot be undone by any subsequent digital operations on the digitized and aliased waveform. For example, subsequent digital filtering of the sampled waveform with a cutoff frequency of 1 kHz will only reduce the noise-to-amplitude ratio to about 45 μV rms. On the other hand, passing the original data through an analog filter with an f_c value 1 kHz would have reduced its amplitude to 3.16 μV rms. There are two possible solutions to this problem: either sample the data at a much higher rate (here at least 2 MHz), or, if the original 10-kHz sample rate is desired, use an analog antialiasing filter prior to sampling which will reduce the amplitude of all frequency components above 5 kHz to an acceptably small level.

In the patch voltage clamp at frequencies above a few kilohertz the PSD of the noise is not flat, but instead rises with increasing frequency, eventually approximately as f^2. In this situation the consequences of aliasing can be even worse than those considered in the previous example. Consider a voltage noise source of 10 nV/Hz$^{1/2}$ in series with a capacitance of 10 pF. In a 100-kHz bandwidth this would result in a current noise of 11.4 pA rms; assume that 100 kHz is the highest frequency of this current noise process. Once again assume that this noise is sampled at a rate of 10 kHz with no antialiasing filter. This will mean that all of the noise above 5 kHz will be aliased into the frequency range from dc to 5 kHz, that is, the sampled data will still have an amplitude of 11.4 pA rms (and an altered PSD), even though the original noise process would only have had an amplitude of about 0.13 pA rms in a bandwidth from dc to 5 kHz. In addition, subsequent digital filtering of the sampled noise with a cutoff frequency of 1 kHz would only reduce its amplitude to about 5 pA rms. However, analog filtering of the original noise with a filter cutoff frequency of 1 kHz would have reduced the noise to about 0.011 pA rms, that is,

more than 400 times less than achieved by digital filtering of the aliased digitized waveform. Once again, much faster sampling or the use of an appropriate antialiasing filter is the solution to this problem.

In the examples presented above it has been assumed that the filter used had a very sharp cutoff beyond its −3 dB bandwidth. As already described, such filters have very undesirable time domain characteristics. When using Gaussian or Bessel filters, which have much more gradual roll-offs beyond f_c, as antialiasing filters it is not appropriate to set f_c equal to f_n. The requirement to avoid significant aliasing and preserve the shape of the original PSD in the frequency range from 0 to f_n is that all frequency components higher than f_n must be adequately attenuated. When using a 4- or 8-pole Bessel filter for antialiasing, the selection of the cutoff frequency, f_c, relative to f_n should take into account the spectral characteristics of the noise as well as just how much aliasing can be tolerated. We advise that at most $f_c < 0.5f_n$ ($0.25f_s$); we typically use $f_c \simeq (0.2-0.4)f_n$.

Cascaded Filters

Care must be taken when two "filters" are used in series. For two Bessel filters, the composite frequency f_c is approximated by

$$1/f_c^2 = 1/f_1^2 + 1/f_2^2$$

This relationship is a reasonable approximation for other filters whose roll-offs are not very steep. Therefore, a resistive headstage patch clamp with a 20-kHz inherent bandwidth filtered by a 10-kHz Bessel filter will result in a bandwidth of about 8.9 kHz. That same patch clamp when recorded by a tape recorder through the 10-kHz Bessel filter and then replayed through a 5-kHz Bessel filter would have a final bandwidth of about 4.4 kHz. It is important not to overlook this result of cascading filters. This problem is a little less severe with integrating patch clamps owing to their high inherent bandwidth, which can easily be 50–100 kHz. A 100-kHz patch clamp filtered through a 10-kHz Bessel filter will have a final bandwidth of about 9.95 kHz, very close to that of the filter itself.

Tape Recorder

For the measurement of steady-state single-channel currents, it is often convenient to use a tape recorder. Up until the last few years, this required instrumentation-type tape recorders that could be very expensive and have quite limited bandwidth. If they had bandwidth, they would go through a great deal of tape to achieve that bandwidth since the tape had to be moved by the recording heads at high speed.

Bezanilla[15] described a technique for using a digital audio processor (DAP) and a standard high-fidelity video tape recorder (home electronics) to do a high quality analog recording. These devices have become so popular that they can now be obtained commercially from a number of different manufacturers. They, in general, sample at 44 kHz, can with some kinds of electronic filtration support up to 20 kHz of continuous bandwidth, and contain from 2 to 8 channels. For the Bessel or Gaussian filters used for patch and whole-cell clamping (see section on filters above), one must sample at 4–5 times the corner frequency in order to eliminate aliasing and to produce data optimal for single-channel analysis. Therefore, the data to the tape recorder must be filtered through a Bessel filter of not more than 9–10 kHz. If measurements are to be made in the frequency domain, sharp roll-off elliptical filters of up to 20 kHz can be supported by the 44-kHz sampling rate of the recorder. These recorders are generally 14- to 16-bit digital devices that use standard video cassettes for their recording, each cassette holding up to 1.5 gigabytes of 16-bit data. For channel current recordings that last up to several minutes, this may be the instrumentation of choice. This technology is now being challenged by computer-based systems with "tape recorder" software (see, e.g., Axotape from Axon Instruments, Foster City, CA).

Computer

Many kinds of patch clamp recording are simply not possible to do adequately without computer control. Many, if not most, channels show transient behavior on switching from one voltage to another. These transients are often finished within 1 to 100 msec after a voltage step, and so this behavior is lost on systems that are tape recorder based and look at only steady-state behavior. To measure this transient behavior, it is necessary that the voltage steps be applied to the patch clamp from digital-to-analog converter hardware located in a computer and that essentially simultaneously the currents coming from the patch clamp be digitized by an analog-to-digital converter also residing in the computer. Many computer systems with real-time interface hardware aimed specifically at this task are now commercially available. The majority of the systems utilize either PC/AT or Macintosh compatible hardware.

One of the newest and most capable systems runs on an Atari microcomputer. Many of these systems use computer graphics hardware to allow

[15] F. Bezanilla, *Biophys. J.* **47**, 437 (1985).

whole-cell currents and single-channel currents to be visualized in essentially real time on the screen of the computer terminal. Some of these systems are beginning to approach the resolution of analog and digital oscilloscopes. The majority of the systems have several channels of analog-to-digital converters and several channels of digital-to-analog converters used to sense the configurations of the patch clamps and to deliver control signals to the electronics, respectively. Some patch clamp manufacturers have implemented "sender" outputs so that the position of key switches like gain switches, filter bandwidth switches, and configuration switches can be read by the computer and stored with the data files being collected. Needless to say, it has become impossible to do state-of-the-art whole-cell recording and single-channel recordings without a system allowing on-line computer support.

Several of the companies that provide hardware support also provide quite complete software packages for the analysis of both whole-cell currents and single-channel currents collected through the use of their interface and computer systems. Consequently, a user getting into patch clamping today has far less to do to be up to speed technically with the field than was necessary a few years ago. These systems all contain software so that raw data files can be reduced, placed in attractive plot format, and plotted on a laser printer to often produce figures that are of publication quality. Anyone getting into patch clamping in the serious way will want to consider the purchase of one or more of these computer hardware and software systems.

Oscilloscope

In addition to the computer display, it is often useful to have a standard oscilloscope connected to the patch clamp output. These instruments provide much greater resolution than computer displays and allow easy change of gain and sweep speeds. One difficulty with standard oscilloscopes is that the screen persistence is short, and so channel currents appear briefly and are not retained. Within the last few years it has become possible to purchase quite inexpensive, digital oscilloscopes that utilize analog-to-digital converters and digital-to-analog converters and internal memory to produce a storage capability not possible with technology that simply alters the screen persistence. Virtually all major oscilloscope manufacturers now produce inexpensive digital oscilloscopes. These are particularly valuable for patch clamp setups because they can at one moment be operated in analog mode and used for all of the electronic purposes that oscilloscopes are good for and then with the push of a single front panel

control provide the digitally derived persistence necessary for optimal viewing of single-channel currents.

Summary

It should be obvious that there are many ways to construct clamp setups that are either equivalent or sufficient for the experiments planned. The hardware and electronics can be obtained from several manufacturers, as can analysis software. What we have presented here are guidelines primarily meant to point a new experimenter in the right direction and, we hope, to guide more experienced investigators toward techniques that can improve the resolution of their measurements.

[3] Glass Technology for Patch Clamp Electrodes

By JAMES L. RAE and RICHARD A. LEVIS

Introduction

In the simplest sense, a patch clamp electrode is just a fluid bridge of proper geometry to connect a reference electrode to the surface or interior of a cell. The glass envelope which accomplishes this is a passive component of the overall circuit which records currents and applies voltages, yet the properties of the glass electrode can be an important determinant of the quality of the recordings.

Several properties of glasses are important when trying to construct effective electrodes for patch clamping. Thermal properties dictate how easily desired tip shapes can be produced and determine the extent to which the tips can be heat polished. Optical properties determine if the tip can be heat polished to a visually distinct end point. Electrical properties determine the noise the glass produces in a recording situation and determine the size and number of components in the capacity transient following a change of potential across the pipette wall. Noise and capacitance properties are correlated. Good electrical glasses minimize both. Finally, glasses are complex substances composed of many compounds (see Table II). Glass composition may influence how easily a glass seals to membranes but may also yield compounds that can leach into the pipette filling solution to inhibit, activate, or block channel currents.

In this chapter, we expand the present literature concerning patch